December 2014 Report: EP201310203080

NAM

Nederlandse Aardolie Maatschappij

Halite dissolution modelling of water injection into Carbonate gas reservoirs with a Halite seal

Table of Contents

Nederlandse Publiekssamenvatting

Schoonebeek productiewater wordt geïnjecteerd in leeg geproduceerde gasvelden (Tubbergen-Mander, Tubbergen en Rossum Weerselo) in Twente. Het water wordt geïnjecteerd in kalksteen (Carbonaat) reservoirs met een boven- en onderliggende afsluitende steenzout (Haliet) laag. Tussen het Carbonaat en het Haliet is een niet doorlaatbare en onoplosbare Anhydriet laag aanwezig.

Het Schoonebeek productiewater is weliswaar zout maar is niet met zout verzadigd. In de MER is uitvoerig aandacht besteed aan het mogelijk oplossen van de afdekkende steenzoutlaag indien deze laag in aanraking zou komen met het injectiewater. De MER concludeert dat deze zoutlagen niet of nauwelijks zullen oplossen in het injectiewater, echter om hierover aanvullende inzichten te verkrijgen is op verzoek van Staatstoezicht op de Mijnen besloten uitgebreide modelleringen uit te voeren.

Op basis van deze uitgebreide modelleringen is aangetoond dat de conclusie uit de MER juist is. Zoutoplossing kan namelijk alleen gebeuren als aan twee heel specifieke condities voldaan kan worden; [1] het injectiewater moet in direct contact kunnen komen met het zout en [2] het injectiewater moet in voldoende mate langs het zout kunnen doorstromen om steeds weer “vers” (niet zout verzadigd) water aan te voeren. Het blijkt dat alleen wanneer injectiewater langs de buitenzijde van de stalen verbuizing van de waterinjectieput zou kunnen stromen, het theoretisch niet uitgesloten kan worden dat de zoutlaag plaatselijk aangetast wordt.

Uit een beschouwing van de putten, waarin het water wordt geïnjecteerd, in samenhang met de geologie van de diepe ondergrond (de Carbonaat laag met de onder- en bovenliggende Haliet laag en de Anhydriet laag daartussen), konden slechts enkele specifieke scenarios geïdentificeerd worden waarbij in theorie injectiewater langs het zout kan stromen. Deze theoretische scenario’s zijn hieronder beschreven en verder toegelicht.

Scenario 1: Dichtbij de put

Direkt rondom een put zou injectiewater dat op diepte van de Carbonaat laag (figuur 1 laag C) wordt geïnjecteerd via mogelijke scheurtjes in het cement dat zich rondom de verbuizing bevindt, waarbij dit cement tevens van slechte kwaliteit is, langs de Anhydrietlaag (A) naar de onder- of bovenliggende zoutlaag (H) kunnen stromen. Daarnaast kan het injectiewater ook in contact komen met het zout als er een lekkage in de ondergrondse verbuizing is ontstaan (zie figuur 1). Afzonderlijk van elkaar kunnen deze situaties niet tot daadwerkelijke zoutoplossing leiden omdat het niet verzadigde injectiewater niet rond kan stromen. Het water raakt daardoor snel verzadigd en raakt daarmee dus snel haar zoutoplossend vermogen kwijt. Slechts een combinatie van deze twee situaties kan theoretisch een continu stromingspad opleveren dat mogelijk tot enige aantasting van de zoutlaag zou kunnen leiden.

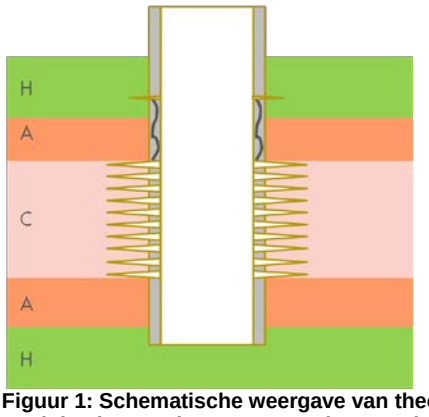

Figuur 1: Schematische weergave van theoretische scenarios waarbij dichtbij de put injectiewater in contact zou kunnen komen met het Haliet (H):

(a) via injectie in het Carbonaat (C), waarna het via mogelijke scheurtjes in cement van slechte kwaliteit rondom de verbuizing langs de Anhydrietlaag (A) stroomt en met het Haliet in aanraking komt

(b) via een lek in de verbuizing ter hoogte van het Haliet

Scenario 2: Op afstand van de put

Als er in het gesteente geen breuken aanwezig zijn, dan kan op afstand van de put door de aanwezigheid van onoplosbare Anhydriet lagen tussen het Carbonaat en het Haliet geen contact ontstaan tussen het injectiewater en het Haliet. Als er echter breuken aanwezig zijn, dan kan een Carbonaat laag toch in contact staan met een Halietlaag (zie figuur 2) doordat de verschillende lagen langs de breuk in diepte zijn verschoven.

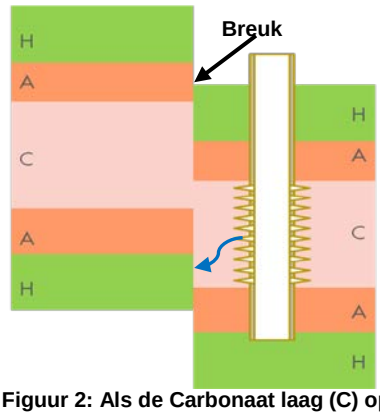

Figuur 2: Als de Carbonaat laag (C) op afstand van de put door verschuiving langs een breuk in diepte overlapt met het Haliet (H) kan injectiewater in direct contact met het Haliet komen

Als dergelijke breuken aanwezig zijn in het gesteente in de diepe ondergrond zou injectiewater op afstand van de put via deze breuken langs het zout kunnen stromen en kan dit tot lokale oplossing leiden. Echter, om het zout op te lossen moet het water vervolgens wel langs deze breuken kunnen wegstromen. Als dit niet zo is, vindt er geen aanvoer van onverzadigd injectiewater meer plaats en raakt het water dat in contact is met het zout snel verzadigd waardoor het zout niet meer oplost. De mate waarin het water langs het zout kan stromen is sterk afhankelijk van de verhouding tussen de horizontale en verticale doorlaatbaarheid (permeabiliteit) van het gesteente (Kv/Kh). Op basis van geologisch inzicht is bepaald dat deze verhouding tussen de 10-3 en 10-4 ligt wat inhoudt dat de de verticale stroomsnelheid van het injectiewater in het gesteente heel laag is waardoor eventuele zoutoplossing ernstig bemoeilijkt en in hoge mate vertraagd wordt.

Het injectiewater zou zich over verloop van tijd kunnen gaan verzamelen op diepere plaatsen aan de rand van het oude gasveld. Als dit water daar in contact zou kunnen komen met een Haliet laag (langs een breuk) zou het daar ter plekke zout op kunnen lossen. In alle analyses is aangenomen dat de initiele zout concentratie van het injectiewater 1.000 ppm is, terwijl voor volledig zout verzadigd water een concentratie van 300.000 ppm aangenomen is. Het met zout verzadigd injectiewater is zwaarder waardoor het door de zwaartekracht naar naar beneden zal zinken. Hierdoor zou het lichtere minder verzadigde water naar boven geduwd worden, waardoor het weer zout zou kunnen oplossen. Als een dergelijke rondstroming zou kunnen optreden (een convectie cel) zou op termijn langs de breuk zout kunnen lossen. Modelleerwerk heeft echter aangetoond dat het minimaal 8000 jaar duurt voordat een dergelijk convectie patroon gevormd kan worden waardoor eventuele zoutoplossing heel erg vertraagd wordt.

Conclusies

Uit het modelleren van het oplossen van steenzout door injectiewater blijkt dat deze zoutlagen niet of nauwelijks zullen oplossen in het injectiewater. Deze conclusie komt overeen met de reeds geconstateerde bevindingen zoals destijds zijn beschreven in het milieueffectenrapport (MER) van Schoonebeek.

De modellering toont aan dat door de lage verticale doorlaatbaarheid (permeabiliteit) van het gesteente het zeer onwaarschijnlijk is dat op afstand van de put, bij een breuk, injectiewater met voldoende hoeveelheid langs het zout kan stromen om het op te lossen. Deze zelfde eigenschap van het gesteente zorgt er ook voor dat de vorming van vloeistofconvectie cellen sterk wordt vertraagd (duurt minimaal 8000 jaar) of zelfs helemaal niet tot stand komt.

Alleen in het geval dat injectiewater gedurende lange tijd langs de buitenzijde van de stalen verbuizing van een waterinjectieput zou kunnen stromen, kan het theoretisch niet uitgesloten worden dat de zoutlaag plaatselijk aangetast wordt. Om een dergelijke situatie te voorkomen is een uitgebreid ‘monitoring plan’ opgesteld dat erin voorziet dat een eventueel lekkagepaden en stroming achter de verbuizing van de injectieputten, ter hoogte van Haliet en Anhydrietlagen, vroegtijdig geidentificeerd wordt zodat tijdig de noodzakelijke mitigerende maatregelen getroffen kunnen worden.

1. Summary

In this report Halite dissolution modelling is being discussed, which has been performed to check the dissolution effects of low saline water injection into depleted Carbonate gas reservoirs containing a Halite cap and base rock. NAM is currently re-injecting low saline production water from the Schoonebeek Oilfield into the Tubbergen and Rossum-Weerselo depleted gas fields, which have above described geological set-up.

In the original Environmental Impact Assessment, a lot of attention was dedicated to the risk of degrading cap rock integrity through salt dissolution. The EIA concluded that this risk is very low. Nevertheless, the Dutch regulator (State Supervision of Mines) requested to do a further and more detailed study into the risk and possible effect of the injection of this low saline water on the cap rock integrity

Halite dissolution can only occur when low saline injection water is able to connect to and flow directly past Halite rock. A review of the injection well design and the injection reservoir geology, identified that there may only be a few very specific situations where such a “Halite flow past scenario” could occur, namely:

1. Near-wellbore cases

In and around an injection well two conditions should be met at the same time to create a possible flow-by scenario: [1] because of a poor cement bond a hydraulic connection should exist between the Carbonate reservoir and the overlying Halite seal via cracks in the production casing cement. [2] In the same interval there should be a leak in the production casing.

2. Far-field cases

In un-faulted areas, contact between the injection water and Halite formations is highly unlikely in view of the presence of continuous anhydrite layers, which shield off the Carbonate injection reservoir from the over- and underlying Halite formations. In faulted areas Halite rock may be juxtaposed against the Carbonate injection reservoir provided the fault offset exceeds the thickness of the over/underlying anhydrite formation (Ref NAM Report: EP201310201845).
In a faulted area a “Halite flow past scenario” could occur when injection water flows laterally from the injector to the juxtaposed Halite rock where it can dissolve some of the Halite. However, in order to cause any significant dissolution, the water needs to flow vertically away from the Halite/Carbonate interface in order to allow a continuous supply of relatively fresh (low saline) water towards the exposed Halite rock.

Another far field “Halite flow past scenario” could occur in a faulted area at the down-dip flanks of the injection reservoir. In these down-dip flanks low saline water could collect over time. In case this injection water contacts any overlying Halite rock, exposed due to faulting, then a convection loop could occur. In this loop, injection water may dissolve overlying Halite rock after which it sinks due to gravitational forces. This may allow less dense injection water to rise from the bottom of the injection reservoir to the exposed overlying Halite rock.

The Halite dissolution modelling results show that the “Halite flow past scenario” could occur under very specific conditions near an injection well. There is however an extensive well monitoring program in place to ensure that occurrence of such conditions is avoided or detected early (Ref NAM Report: EP201410210164).

For the far-field cases the Halite dissolution modelling results show that the “Halite flow past scenario’s” are not likely to cause significant dissolution, because of the very low vertical communication within the injection reservoir. The presence of anhydrite layers in the carbonate injection reservoir result in very low K_v/K_h ratio’s (in the order of 10^{-3} to 10^{-4}). Close to fault zone, where halite may be juxtaposed against reservoir Carbonates, this means that any low saline injection water cannot flow away fast enough to cause significant dissolution. The same reservoir property will also prevent the formation of fluid convection loops at reservoir scale (i.e. 50m thickness). Simulations show that it will take 8000 to 75000 years for a convective loop to develop. It is also shown that even if it develops, the dissolution capacity is very limited.

The modelling studies of the Twente Carbonate reservoirs fully supports the conclusion from the original EIA in that the risk for significant halite dissolution is expected to be very low.

2. Modeling assumptions

Within the Schoonebeek Oilfield production system low saline production water is being re-injected into several depleted gas fields in Twente. Two of these fields, Tubbergen (TUB) and Rossum-Weerselo (ROW), have injection reservoirs which are sealed off by Halite formations. Modeling has been performed to study potential dissolution effects of the injected low saline water on these Halite formations. In order to put the modelling work conducted in this study in context a brief background is given of the geology of the TUB and ROW fields, the multi-phase flow behaviour within their reservoir intervals and the nature of halite dissolution in water.

2.1 Geology of the Tubbergen and Rossum-Weerselo water injection fields

A geological review of the Tubbergen (TUB) and Rossum-Weerselo (ROW) injection reservoirs has been performed. In this section some of the key conclusions from this review will be repeated.

In the TUB and ROW fields the injection reservoirs are the ZEZ2C and ZEZ3C Carbonate layers in the Zechstein formation and the DC sandstone in the underlying Limburg formation. The Carbonate injection layers in these fields have a Halite/Anhydrite top and base seal whereas the seal of the DC sandstone is formed by intra Carboniferous shales and base Zechstein Anhydrites (Werra Anhydrite). Halite dissolution modelling therefore has been focussed on the Carbonate injection reservoirs.

The Zechstein formation in the TUB and ROW fields consists of the regional 4 evaporitic cycles (i.e. deposition in each cycle consisting of a sequence of Clay-Carbonates-Anhydrites-Salts and Halites/Anhydrites), whereby the 4^{th} cycle may not be developed fully (only Halites developed mainly). Gas has been produced from the Carbonates in the 2^{nd} and 3^{rd} cycle, also called ZEZ2C and ZEZ3C. After conversion of the TUB and ROW wells to water injectors water is therefore being injected in the ZEZ2C and ZEZ3C Carbonates.

The Z2 and Z3 reservoirs are, in general fairly conformal and separated by uniformly thick halite and anhydrite layers. There is a very good correlation of these anhydrite layers between all wells in the TUB and ROW field as well as regionally. It is therefore clear that the anhydrite layers are developed regionally and hence can be assumed to be present across the entire TUB and ROW fields.

The ZEZ2C and ZEZ3C Carbonates are, in general, characterized by dolomitic layers interspersed by Anhydrites. In the ZEZ3C Carbonates these dolomitic layers are typically 20-30 cm thick whereas the interspersed Anhydrites range in thickness from cm to dm. In the ZEZ2C Carbonates the dolomitic and interspersed Anhydritic layers are thicker (both 4-5m).

In both ZEZ2 and ZEZ3 Carbonate reservoirs, the main permeability is provided by the presence of open fractures. Core material shows that the fractures are present in the clean carbonates (Dolomites) and are absent (abut) as soon as an Anhydrite or anhydritic layer is present. The presence of interspersed anhydritic layers within the Carbonate reservoirs therefore means that the fracture networks are laterally quite extensive but vertically limited. This fracture distribution heavily dictates the effective permeability and Kv/Kh on a reservoir scale. The conducted geological review concluded that the Kv/Kh ranges from 0.005 for an un-faulted area to 0.0001 for areas, affected by fault associated fractures.

To build a representative reservoir model for Halite dissolution, it is important to know the fracture density within the Carbonate reservoir. This fracture density is determined from fracture network porosity and fracture aperture. We assume a fracture porosity range of 0.25% to 1% with the upper bound corresponding to the fracture porosity used to achieve a good history match to gas production data. For the fracture aperture, a range of 5×10^{-4} m to 2×10^{-3} m (0.5 mm to 2 mm), based on core observations, is assumed. From these assumptions the fracture density is calculated in the range of 2.5 fractures/m^3 to10 fractures/m^3 where we define fracture density as the number of fractures per cubic meter of gross rock volume (solid rock plus fractures). If we assume that the fractures are only present in one dimension then the fracture spacing ranges from 0.1 m to 0.2 m. If the fractures exist in two dimensions then the fracture spacing ranges from 0.2 m to 0.4 m. The absolute permeability through a fracture is also uncertain; here we assume a range of 25 D to 250 D.

Whether the fracture network exists in one- or two-dimensions is difficult to predict. In general the present day horizontal stress distribution would predict a maximum horizontal stress orientation of

NW-SE, with open fractures aligning along this direction. However, since the Zechstein carbonates are embedded in salt they have their own stress field (due to faulting/bending/folding) caused by salt movement, and therefore their own fracture orientation. For the TUB and ROW fields, due to the presence of salt, we can assume that fractures are present in two directions. Figure 2.1 illustrates the 2-D fracture orientation assumption for TUB and ROW and Table 2.1 summarises the typical ranges of geological input parameters considered in this study.

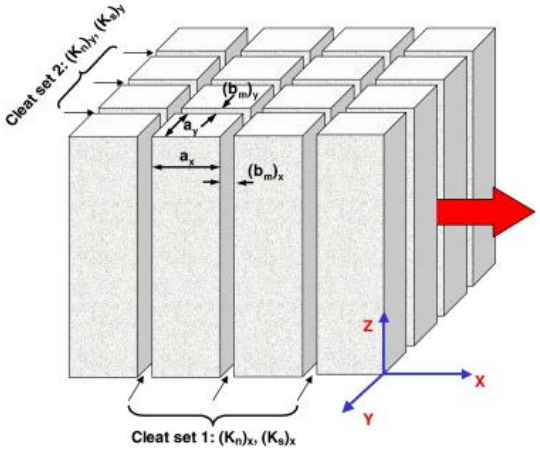

Figure 2.1: It is assumed that fracture planes exist in the X and Y directions in the TUB and ROW fields. Properties of the dual-porosity formation include: the fracture spacing $a_{x,y}$ and the fracture aperture $(b_m)_{x,y}$. Figure reproduced from (Permeability and porosity models considering anisotropy and discontinuity of coalbeds and application in coupled simulation, 2010).

Table 2.1: Range of Zechstein carbonate properties associated with matrix and fractured pore systems (range covers both 1D and 2D fracture geometries).

Zechstein Carbonate Reservoir Property	Range	Base Value
Matrix Porosity	1-6%	3%
Matrix Permeability (mD)	0.1 - 10	0.1
Absolute Fracture Permeability (D)	25-250	25
Fracture aperture (mm)	0.5-2.0	1.0
Fracture Porosity	0.25-1%	1%
Matrix block dimension (m)	0.1 – 0.4	0.2
Effective Medium Permeability (mD)	13-2500	177

2.2 Water injection behaviour in depleted dual porosity gas reservoirs

In 2004 water injection into depleted Zechstein group gas reservoirs was studied in detail (Weijermans, 2004). The primary focus of the study was to understand the long term injectivity capacity of the fields, but the fundamental behaviour of the displacement process was also investigated. We will recap some of that work here before discussing our own modelling work.

In a fractured (dual porosity) reservoir the flood front between injection fluid and reservoir fluid is controlled by the fluid properties and the reservoir properties. Two general behaviours can be considered; fracture constrained, and matrix constrained. In a fracture constrained system the injectivity capacity of the fracture system is limited and therefore the reservoir behaviour is similar to that of a single porosity system: a stable flood front propagating away from the injection well. In a

matrix constrained system there is a constraint on the matrix-fracture fluid transfer and hence the flood front progresses further in the fracture system than in the matrix system, this is illustrated in Figure 1.2.

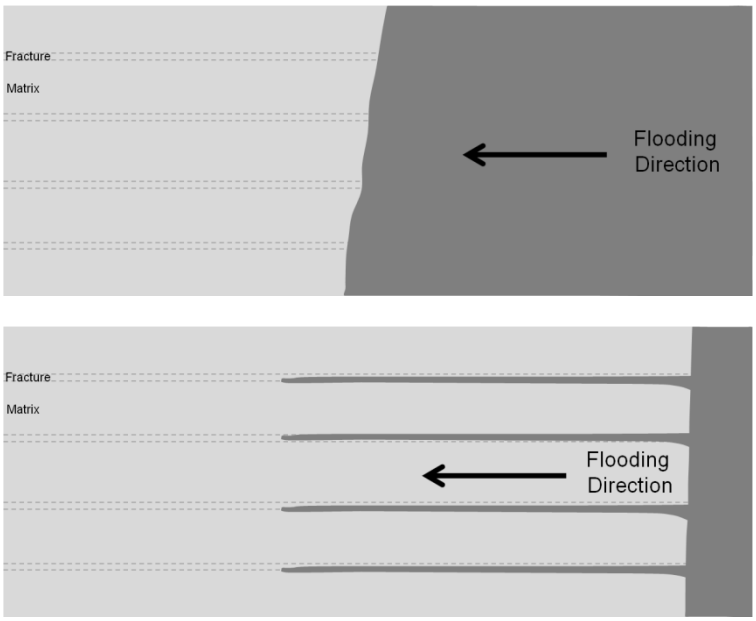

Figure 2.2: Schematic representation of fracture (top) and matrix (bottom) constrained flood front behaviour in a dual porosity system. The light grey colour represents the pore space filled with gas, the dark grey colour is pore space containing injected water. In the fracture constrained system the flood front behaves in a similar manner to a single-porosity system. In the matrix constrained system the flood front in the fracture network advances ahead of the flood front in the matrix.

To understand whether the system is fracture or matrix constrained the Zechstein Carbonate dual porosity system was modelled using an approach which has been introduced by Hagoort (2003) (Weijermans, 2014). In this approach a dual porosity system is modelled as a single porosity system. Herewith the permeability of the equivalent single-porosity reservoir is equal to the effective fracture permeability of the dual-porosity reservoir. To account for the dual porosity nature a dual porosity skin Sdp has been introduced into this single porosity model. If the pseudo-skin is negligibly small, the system is limited by the capacity of the fracture system and the PI is equivalent to the PI of the single porosity reservoir model using the effective fracture permeability. If the pseudo-skin is large, the PI is constrained by matrix-fracture fluid transfer and the PI can be much lower than the PI of the equivalent single-porosity model (using the effective fracture permeability). Therefore we can use the dual-porosity skin as a dimensionless number to characterize the situation, i.e. to determine whether the dual porosity system is matrix or fracture constraint.

The dual porosity skin is given by:

$$s_{DP} = \frac{2(k_e / k_m)(1-\omega)^2}{\sigma r_e^2} \qquad (1)$$

where:
k_m= matrix permeability
k_e= effective medium permeability
ω = storativity ratio
r_e= external radius
σ = shape factor

and the storativity ratio is defined as:

$$\omega = \frac{\phi_f c_f}{\phi_f c_f + \phi_{ma} c_{ma}} \qquad (2)$$

where:

ϕ_f =effective fracture porosity
ϕ_{ma} = matrix rock porosity
c_f = compressibility fracture system
c_{ma} = compressibility matrix rock

We assume nearly equal compressibility of matrix and fracture systems reducing equation 2 to:

$$\omega = \frac{\phi_f}{\phi_f + \phi_{ma}} \quad (3)$$

and shape factor is given by:

$$\sigma = \frac{\pi^2}{L^2} \quad \text{for a 1-D fracture system} \quad (4)$$

$$\sigma = \pi^2 \left(\frac{1}{L_x^2} + \frac{1}{L_y^2} \right) \quad \text{for a 2-D fracture system} \quad (5)$$

$$\sigma = \pi^2 \left(\frac{1}{L_x^2} + \frac{1}{L_y^2} + \frac{1}{L_z^2} \right) \quad \text{for 3-D fracture system} \quad (6)$$

where $L_{x,y,z}$ are the matrix block length dimensions.

Based on equations (1) – (6) the dual porosity skin can be plotted as a function of matrix block size (determined by the matrix block length dimensions $L_{x,y,z}$) and the ratio k_e/k_m with k_e as the effective medium permeability and k_m as the matrix permeability. This figure also shows a region, which has been annotated with ZEZC, to represent the range of parameters (Matrix block dimensions, k_e and k_m) that have been encountered in the Zechstein Carbonate. The parameters for the ZEZC have been calculated in section 2.1 and are summarised in Table 2.1.

Comparing the region typical for the ZEZC with the S_{dp} contour lines shows that the Zechstein Carbonates have a very low dual porosity skin S_{dp}. This means – as explained at the start of this section – that the system is fracture constraint. Further modelling work to investigate salt dissolution is therefore performed on a single porosity grid system for simplicity and to save computational time.

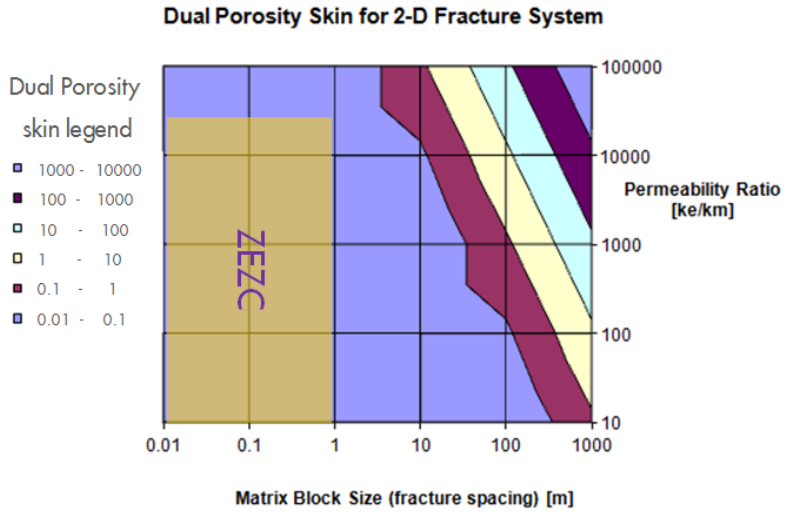

Figure 2.3: Contour plot of dual porosity dimensionless skin (Eqn. 1) as a function of permeability ratio and matrix block size. Conditions pertinent for the ZEZC have been indicated with a grey box.

2.3 MORES model assumptions

In this section additional modelling assumptions are described which are used in the simplified single porosity model used for modelling halite dissolution. The geological input parameters (e.g. porosity, permeability) are described in section 2.1 and are not discussed again here. In the subsequent section 2.4 we will describe the MoReS input language that allows us to model halite dissolution.

2.3.1 Porosity and permeability

The geology of the Tubbergen (TUB) and Rossum-Weerselo (ROW) gas fields is described in section 2.1. The dissolution modelling uses a simplified single-porosity model and we assume the porosity is equal to the dual-porosity matrix porosity (3%), i.e. fracture pore volume is negligible compared to matrix pore volume. It is necessary to average the matrix and fracture permeability to reach representative effective single-porosity permeability for use in the model. We consider fractures that are parallel to the flow direction and ignore perpendicular fractures (the increase in average permeability due to flow across a very small fracture aperture – flow in series – is negligible when averaged harmonically). We use the arithmetic average of the matrix and fracture permeabilities for flow in parallel:

$$\bar{k} = \frac{\sum_{j=1}^{n} k_j h_j}{\sum_{j=1}^{n} h_j} \qquad (7)$$

where $\bar{k}$ is the arithmetic average permeability, n = 2 (fracture or matrix), and k_j and h_j the permeability and thickness in layer j respectively. An arithmetic averaging of the input assumptions, summarised in Table 2.1, results in an effective medium permeability in the range 13-2500 mD.

2.3.2 PVT and salinity

The aqueous phase salinity is modelled explicitly and is accounted for in the SIMDATA.SLT array, the functionality is activated using `USE_GRIDBLOCK_SALINITY = ON`. This flag triggers continuous updating of water density and viscosity for every gridblock based on its salinity, pressure and temperature. We specify an initial salinity in EOSDATA (`eclModel SALINITY = …`). The salinity is tracked through the use of a passive tracer and the salt is not a separate component; the model is therefore two phase (water, gas) two component (H_2O, CH_4). We include an Eclipse format EOS file (`eclModel ECL_FILE`) describing a single component (CH_4) gas phase. The salinity of the injected water is assumed to be 1000 ppm and the maximum salinity at reservoir conditions (the salinity of connate formation water) is assumed to be 300,000 ppm (unit: ppm = 10^6·(mass of dissolved salt)/(brine mass)). Due to flow induced water mixing (modelled using the passive tracer), intermediate salinities will develop during the simulation.

2.3.3 Gridding

The choice of model (2D radial, 3D box) and grid cell sizes depends on the dissolution problem under investigation. These scenarios can be broadly grouped into near wellbore and far-field cases and are described in more detail in section 3. Both box models and radial models are used. While the lateral grid extent varies depending on the model the grid cell heights are chosen based on the halite solubility, as discussed below in section 2.4.

2.3.4 Saturation curves

For the Tubbergen and Rossum-Weerselo fields there are no saturation curves available from special core analysis data whilst only limited suitable analogue data are available in the RELATE database. Based on previous work (Weijermans, 2004) and the water injection FDP documents (Warren, et al., 2006)) the parameters summarised in Table 2.2 – and plotted in Figure 2.4 – were used in this study. Secondary drainage was not modelled in this study.

Table 2.2, Summary of Corey-model parameters used to calculate relative permeabilities as a function of water saturation.

Relative Permeability Corey-Model Parameter	Primary Drainage	Secondary Imbibition
Connate Water Saturation (S_{wc})	0.25	na
Residual Gas Saturation (S_{gr})	na	0.15
Gas end-point relative permeability (at S_{wc})	0.9	0.9
Water end-point relative permeability (at S_{gr})	na	0.5
Gas Corey exponent (n_g)	2	3
Water Corey Exponent (n_w)	4	4

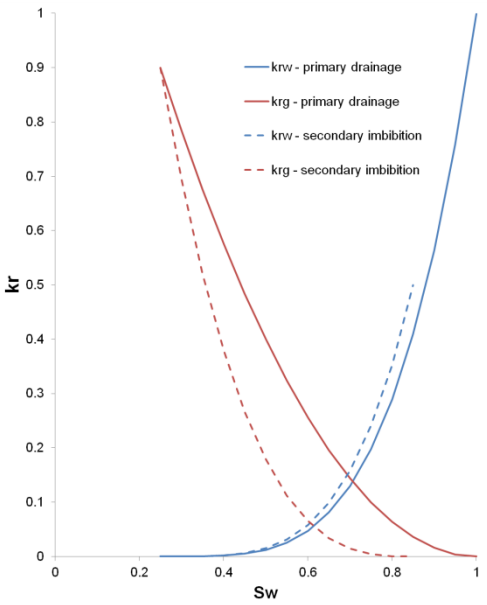

Figure 2.4: Corey-Model primary drainage and secondary imbibition relative permeability curves used in this study (input parameters are summarised in Table 2.2).

2.4 Halite dissolution and implementation in MORES

Halite (NaCl) is soluble in water with the saturation limit and rate of dissolution dependent upon the precise thermo-physical conditions. To get a feel for the magnitude of potential dissolution consider a simple 'worst case scenario' thought experiment: at T = 60 °C 37.1 g of NaCl will dissolve in 100g of water (Dean, 1999). In a worst case scenario a 100 m × 100 m × 1 m reservoir volume (rock volume = 10000 m^3) with a porosity of 5% (pore volume = 500 m^3) filled entirely with pure H_2O would dissolve 185500 kg of halite assuming perfect mixing (37.1 g halite/100 g H_2O; ρ_{H2O} = 1000 $kg.m^{-3}$). This equates to a halite volume of 85.7 m^3. Assuming the halite overlays the entire top surface of the reservoir volume, and that dissolution is homogeneous across that surface, then a halite layer 0.857 cm thick (100 m × 100m × 0.00857 m) would dissolve (ρ_{halite} = 2165 $kg.m^{-3}$).

A constant injection water salinity of 1,000ppm is assumed and a saturation limit of 300,000 ppm for the formation water at reservoir conditions. The injection water salinity is at the lower end of the range expected during the project and therefore represents a 'worse case' assumption.

Two methods of modelling halite dissolution have been developed and implemented in Dynamo-MoReS. Both methods update the salinity of under-saturated water in proximity with halite, but they differ in terms of whether the void space created by halite dissolution is modelled explicitly or

not. Modelling the halite – and dissolution void space – explicitly is computationally expensive and hence the second method was developed in parallel allowing us to model the full range of dissolution scenarios described in Section 3.

2.4.1 Dissolution Method 1: Salinity Update and Explicit Modeling of Halite Void Space

In the first method halite and carbonate layers are modelled explicitly with each layer divided into a number of grid cells. Initially the halite cells are solid (non-porous) and hence do not contain any water or gas. The dissolution of halite and the corresponding increase in water phase salinity is controlled by a monitor which works in a number of logical steps:

1. A search is performed to identify any halite cells which are adjacent to a cell containing under-saturated water (SLT < 300000)[1]. If such proximity exists then the subsequent steps are taken (if not then no action is taken).
2. A mass of salt is passed from the halite cell(s) to the adjacent cell containing the under-saturated water. This results in an update to the SLT array in the receiving cell (proportional to the mass of salt transferred) and in the creation of porosity (the void space) in the halite cell(s)[2].
3. The porosity created in the halite cell(s) is filled with water taken from the adjacent cell that initially contained the under-saturated water.
4. The water now occupying the porosity in the halite cell(s) is assigned the same pressure as the adjacent cell that initially contained the under-saturated water [3].
5. The permeability of the halite cell containing void space is set as a function of the porosity (K = 10 D * φ).

Figure 2.5 illustrates this process for transfer between two cells only; the simplest scenario considered. As described in the steps above (and the footnotes) more than one halite cell could contribute to mass transfer under certain conditions, this could also result in non-vertical mass transfer (e.g. from cell X to cell X+1).

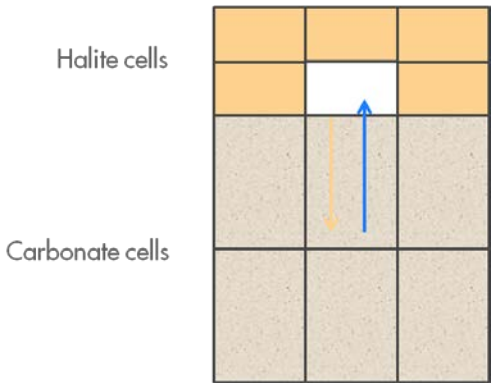

Figure 2.5: Illustration of NaCl mass transfer between a halite cell and a carbonate cell containing under-saturated water.

The advantage of this modelling approach is that an understanding of the shape of the dissolved void space can be gained. As dissolution proceeds we continue to simulate multi-phase flow in the resultant void space, allowing fresh water to access solid halite cells away from the original halite-carbonate boundary. However it is important that the limitations of this modelling approach are

[1] Initially (prior to dissolution) only carbonate cells can contain under-saturated water (as the halite is solid). Over time, as halite dissolves, under-saturated water can occupy the resultant void space. Subsequently halite cells located away from the carbonate-halite interface can also dissolve.

[2] The monitor will attempt to fully saturate the water with salt but it will also take into account the amount of halite available in adjacent cells. If the mass of adjacent halite is limited, i.e. it is less than the amount required to reach full saturation, then the salt transferred is limited accordingly.

[3] By assigning the pressure of the water-filled cell to the newly created pore space in the halite cell it is assumed that the volume change of the aqueous phase (due to salinity change) is equal to the volume of pore space created by dissolution.

also understood. Simulation of flow within the void space is handled with the Darcy solver in Dynamo-MoReS. The constitutive Darcy equations were developed for flow in porous media and therefore the accuracy of the void space results is uncertain. This should be remembered when considering any quantitative analysis of simulated dissolution patterns. Furthermore the complexity of the monitor makes it unstable in certain scenarios; such as when there are large fluxes in small dissolution void spaces.

The monitor described above, and associated other input language, is included in Appendix 1. Note that at this stage the implementation is not robust enough such that one include file is suitable for any deck. Modifications are required to reflect the model type (radial, 2D box, 3D box) and to identify the specific halite layer ranges.

2.4.2 Dissolution Method 2: Salinity Update and Dissolved Halite Mass Tracking

In the second approach dissolution does not occur explicitly – such that void space is created – instead the salinity of the aqueous phase is updated upon proximity with the carbonate-halite interface, and a record is kept of the total mass transfer associated with this salinity change over time. This simpler approach is more stable and less computationally intensive making it more suited for use in larger or full-field models. The implementation is by way of a monitor and other associated input language and the steps taken are given below:

1. A passive tracer is used to account for water salinity in terms of the fraction of fresh water (1000 ppm salinity) and formation water (300000 ppm salinity) in each grid cell. The SLT array is set based on this ratio.
2. The carbonate cells at the carbonate-halite boundary are identified.
3. In each of these cells the degree to which the aqueous phase is under saturated with respect to salt is determined.
4. The salinity is subsequently set to its upper limit (where that is not already the case) and a record is kept of the corresponding mass of halite which would be dissolved for such a mass transfer. In addition the passive tracer is updated to reflect the change in salinity.
5. The final step involves updating the porosity and permeability of the interface cells where mass transfer has occurred. The intention is to account for preferential flow paths which may emerge in the void space created by dissolution[4].

[4] Since the preferential flow paths within the void space created by dissolution are not modelled explicitly the effect in the carbonate cells is averaged. The porosity is increased in line with the halite mass transferred (up to a maximum porosity of 1.0) and a relationship between porosity and permeability is assumed ($K = 10^{400\delta\phi}$), with permeability allowed to increase up to a maximum of 10 Darcy.

3. Halite dissolution scenario's

Based on the geological analysis (NAM report EP201310201845) and discussions with the State Supervision of Mines(SodM) , a number of scenarios were identified that cover the full range of possible conditions that could, in theory, result in halite dissolution.. These can be grouped into near-wellbore and far-field scenarios.

3.1 Scenario 1: Cement crack

Figure 3.1Figure illustrates the case where a poor wellbore cement job – or a region of cracked cement – could act as a potential pathway for injection water to flow from the carbonate formation (indicated by C) past the Anhydrite formation (indicated by A) to halite formations (indicated by H).

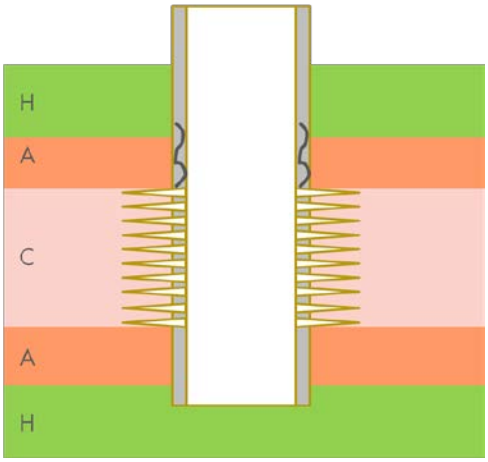

Figure 3.1: Dissolution scenario 1: a poor cement job results in a pathway for water in-between the carbonate and halite layers.

3.2 Scenario 2: Casing leak & cement crack

The scenario whereby the cement crack described in scenario 1 is coupled with a leak point (e.g through corrosion) in the wellbore casing is shown in Figure 3.2. The assumption is that the leak point is small and it is located opposite a halite interval. A crack in the annular cement provides the connection between the carbonate formation and the casing leak point.

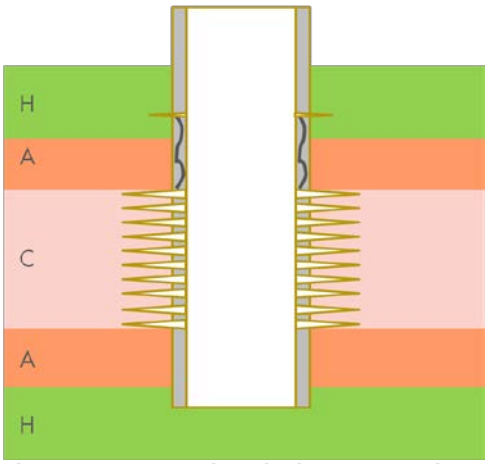

Figure 3.2: Dissolution scenario 2: a leak point exists in the wellbore casing within the halite interval. In-between casing leak point and the carbonate formation there is a crack in the annular wellbore cement.

3.3 Scenario 3: Hydraulic fracture

The third dissolution scenario (Figure 3.3) assumes that injection hydraulically induced fracture is formed in the carbonate and anhydrite formations (the fracture stops at the anhydrite-halite boundary). The fracture is assumed to be a high permeability conduit for flow and it has a fracture half length of 70 m in the anhydrite and 350 m in the carbonate.

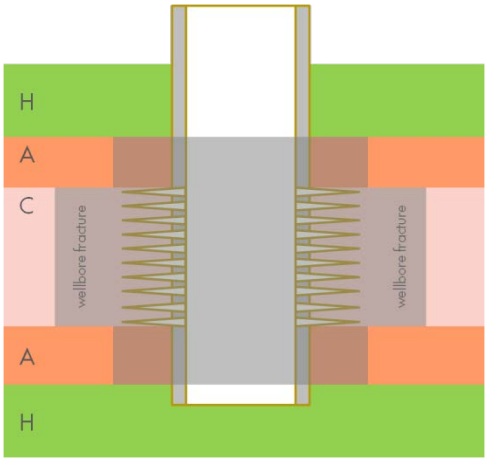

Figure 3.3: Dissolution scenario 3: a vertical planar fracture (represented by the grey shading) extends from the wellbore in the anhydrite and carbonate formations.

3.4 Scenario 4: Water flowing past juxtaposed Halite in faulted areas

Scenario 4 is the first of the far-field cases and envisages the flow of water past a halite layer across a fault (Figure 3.4). The assumption is that the throw of the fault is sufficient to juxtapose a halite layer and a carbonate layer against each other. Injected water that flows across the fault may therefore be in proximity to the exposed halite leading to dissolution.

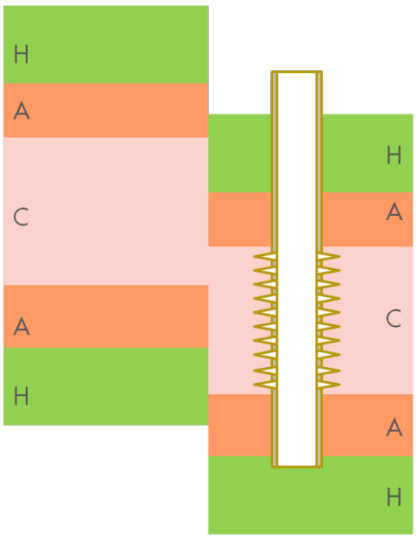

Figure 3.4: Halite and carbonate layers are juxtaposed together across a fault. Injected water that flows across the fault may come into proximity with the halite layer leading to dissolution.

It should be noted that at the fault interface a direct and undisturbed contact has been assumed between the lithologies. In reality a significant reduction in permeability in the Carbonate layers near faults is expected as salt creep causes fractures in the vicinity of the fault to be filled with salt. (ref NAM report EP201310201845) This will reduce cross-flow past faults and will therefore significantly hamper halite dissolution near faults. The results of this modelled scenario therefore represent a very conservative assumption.

3.5 Scenario 5: Convection loops at faulted areas in down-dip flanks of reservoir

During and after injection, injection water could collect in the down-dip flanks of the anticlinal injection reservoir. Here the water in the reservoir could connect direct with overlying Halite at faults that have a larger offset than the intermediate Anhydrite layer, see Figure 3.5. When halite dissolves into water the aqueous phase density increases leading to a gravitationally unstable situation where water of higher density overlies water of lower density, eventually leading to the formation of a convective loop or cell (see figure 3.5).

To simulate this case it is very conservatively assumed that the halite layer is in direct contact with the carbonate formation vertically: i.e. it overlays the carbonate. As a convective cell forms fresh (lower density) brine moves upwards which could lead to further dissolution. Note that the maximum halite thickness dissolved is governed by the amount of fresh water underneath the exposed Halite in the reservoir: i.e. it can be approximated as a function of $H\varphi S_w$, where H is the formation thickness, φ is porosity and S_w is the water saturation.

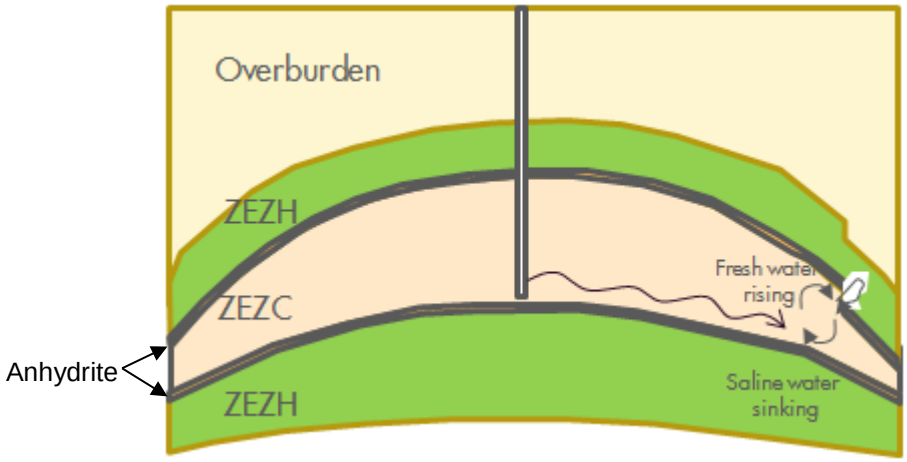

Figure 3.5: Injected water could collect at the down-dip flanks of the anticlinal reservoir where it could contact Halite at faults, which have a bigger offset than the intermediate Anhydrite layers.

4. Dissolution scenario modeling

The dissolution scenarios outlined in section 3 were investigated with a range of modelling approaches utilising the two dissolution scripts detailed in section 2.4.

4.1 Scenario 1: Cement crack

Scenario 1 was modelled in a simple 2D radial model comprising three vertical intervals: a halite, anhydrite and carbonate. The halite and anhydrite layers were initially non-porous and the carbonate layer had a constant porosity of 0.03 and permeability of 125 mDarcy. The halite layer was modelled in fine detail to capture the shape of any dissolved region (50 m halite layer divided into 0.05 m thick halite cells) and the cell radii increased exponentially away from the wellbore, with the first cell having a radius of 0.023 m. Where the annular cement is assumed to be undamaged the permeability and porosity are set to zero, while in the damaged region a permeability of 10 D and a porosity of 0.2 are assumed. Furthermore straight line relative permeability curves are assigned to the damaged region in addition to a constant capillary pressure of zero over the full saturation range ($S_{wc} < S_w < 1.0$). An analytical aquifer allowed for leak off at the outer radius of the model.

Water (1000 ppm salinity) was injected at a rate of 2500 m^3/day for a period of 20 years. The injection well was subsequently closed and a 1000 year shut-in period was simulated.

Any dissolution resulted in porosity and permeability being updated in the halite cells as described in section 2.4.2; up to a maximum of $\varphi = 1$ and $K = 10$ D. These cells were also assigned straight line relative permeability curves and a constant capillary pressure of zero over the full saturation range ($S_{wc} < S_w < 1.0$).

4.2 Scenario 2: Casing leak & cement crack

Scenario 2 was modelled exactly as scenario 1 except for the addition of a single leak point in the well casing located opposite the halite interval. The additional completion corresponded to the upper height of the cracked wellbore cement. In this way a viable flow pathway was introduced from the leak point, through the cracked cement, and down to the carbonate formation. It is assumed that the casing leak area is constant through time (one halite cell is completed with a height of 0.05 m). Furthermore only one height of the leak point within the halite formation is investigated.

4.3 Scenario 3: Hydraulic fracture

Scenario 3 was modelled with a simple 3D box model (see Figure 4.1). Cell heights, porosities, permeabilities (of the un-fractured medium) and injection rate are as described above for scenarios 1 and 2. The hydraulic fracture is assumed to extend over the full height of both the carbonate and anhydrite layers with half lengths of 70 m and 350 m respectively (section 3.3). The fracture was modelled explicitly by setting the middle Y-dir cell width equal to 0.01 m. The other Y-dir cells increased in size away from the model centre where the well was located. The fracture was assigned a porosity of 1.0, a permeability of 10 D, straight line relative permeability curves, and a constant capillary pressure of zero over the full saturation range ($S_{wc} < S_w < 1.0$). Analytical aquifers allowed for leak off in the X and Y directions at the outer model faces.

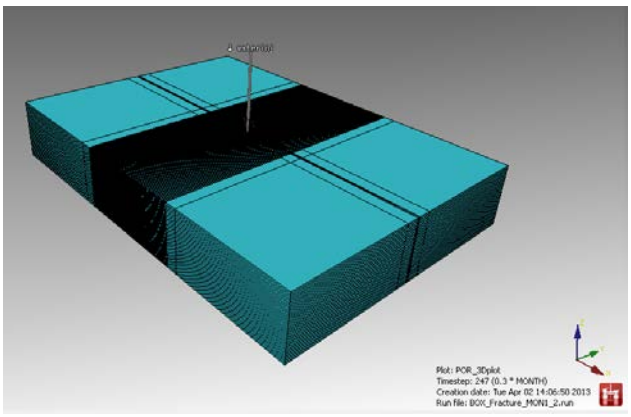

Figure 4.1: Dynamo-MoReS 3D box model used to investigate the impact on halite dissolution of a wellbore fracture through carbonate and anhydrite formations.

4.4 Scenario 4: Water flowing past juxtaposed Halite in faulted areas

Scenario 4 was modelled in a 3D box model which comprised of five layers: halite-anhydrite-carbonate-anhydrite-halite. In one half of the model this sequence was shifted vertically, in relation to the other half, thus representing the throw across a fault. The throw was 35 m, sufficient to juxtapose carbonate against halite laterally. The injection well was located in one fault block with analytical aquifers placed at the boundaries to allow leak off (in X and Y directions). Cell sizes and well location were designed to ensure that injection water would flow across the fault block during the 20 year injection period (2500 m^3/day injection rate) which was followed by a 1000 year shut-in period. Different ratios of vertical to horizontal permeability (K_v/K_h) were investigated.

4.5 Scenario 5: Convection loops at faulted areas in down-dip flanks of the reservoir

Scenario 5 was investigated using both analytical and numerical models, with the objective being to understand the timescale of dissolution and convective mixing. In both cases a number of sensitivity cases were ran to investigate the impact of carbonate layer thickness and K_v/K_h.

The analytical analysis was based on models developed for CO_2 dissolution in brine (Rate of Dissolution due to Convective Mixing in the Underground Storage of Carbon Dioxide, 2003) (Onset of Convection in a Gravitationally Unstable Diffusive Boundary Layer in Porous Media, 2006), which in turn are mathematically equivalent to the well-studied problem of temperature-driven convection in porous media. The analytical analysis gives estimates for the critical time (t_c) – that is the time at which an instability begins to propagate – the dimensional critical wavelength (λ_c) and the penetration depth at the onset of instability (δ_c), assuming that δ_c is much smaller than the domain thickness (H):

$$t_c = 146\frac{\varphi\mu^2 D}{(K\Delta\rho g)^2} \quad (8)$$

$$\lambda_c = \frac{2\pi\mu D}{0.07K\Delta\rho g} \quad (9)$$

$$\delta_c \approx \frac{24\mu D}{K\Delta\rho g} \quad (10)$$

where μ is the fluid viscosity, D the effective diffusivity of salt in the aqueous phase, g is the acceleration due to gravity, and $\Delta\rho$ the density increase due to a salinity change from 1,000 to 300,000 ppm. For the anisotropic permeability cases (K_v/K_h < 1) the above formulas are thought to remain approximately valid if the following permeability definition is used (Rate of Dissolution due to Convective Mixing in the Underground Storage of Carbon Dioxide, 2003):

$$K = \frac{4K_vK_h}{\left(K_v^{\frac{1}{2}}+K_h^{\frac{1}{2}}\right)^2} \quad (11)$$

and hence for $K_v/K_h \ll 1$, $K=4K_v$. Moreover, for nonzero gas saturation, K needs to be multiplied by the water relative permeability.

Numerical models used the second dissolution script (section 2.4.2) in simple 2D and 3D box models. In this scenario the halite was assumed to be in direct contact with the carbonate formation (approximating the case of a faulted area where Halite is juxtaposed against Carbonate). The box models were initialised with a water saturation of 0.8 (typical water saturation on the flank developing after shut-in, obtained from a full field model) and a water salinity of 1,000 ppm. The grid cell sizes were set based on the analytical estimates of the critical wavelength for each of the scenarios simulated. The diffusion constant D was assumed to be 10^{-9} m^2/s (realistic value for CO_2 diffusion in water in a porous medium at the temperature, pressure and porosity of interest)

5. Dissolution scenario results

5.1 Scenario 1: Cement crack

Simulation of scenario 1, where a crack exists in the wellbore annular cement, showed no convective flow over the simulation timeframe. This result is intuitive: no plausible flow path exists from the pressurised carbonate formation up the cracked cement (which terminates as a dead-end). The simulations did show a salinity change in the aqueous phase that occupies the crack over time, specifically the brine in proximity with the halite. This is a diffusive process with the timescale (t) given as $t = H^2/D$; where H is the distance and D is the diffusion constant ($1\times10^{-9}m^2s^{-1}$). It would hence take 3170 years for the salinity to change across an anhydrite interval which is 10 m thick (50700 years across a 40 m thick anhydrite interval), assuming halite is only exposed at one end of the crack and not along its length.

5.2 Scenario 2: Casing leak & cement crack

In scenario 2 the cement crack of scenario 1 is accompanied by a leak point in the wellbore casing adjacent to the halite formation. In this case the radial model simulation predicts the formation of a dissolution zone originating at the leak point. A valid flow path now exists with some of the injection water passing through the leak point and down the cracked cement into the lower pressure carbonate formation. As this water dissolves halite a void space develops. Subsequent water that passes through the leak point has a residence time within the void space allowing further halite to dissolve, resulting in the gradual growth of the void/cavity. The amount of water that passes through the leak point (compared to the total water injection rate) is limited by the conductivity of the cement crack; in our simulations approximately 3% of total injected water passes through the leak point. This amount remains constant throughout the injection period. Throughout the 20 year injection period, the cavity volume grows at a constant rate of approximately 20 m^3/year (Figure 5.1). This is in line with the constant water rate through the leak point. The cavity is expected to have an approximately cylindrical in shape (Figure 5.2).

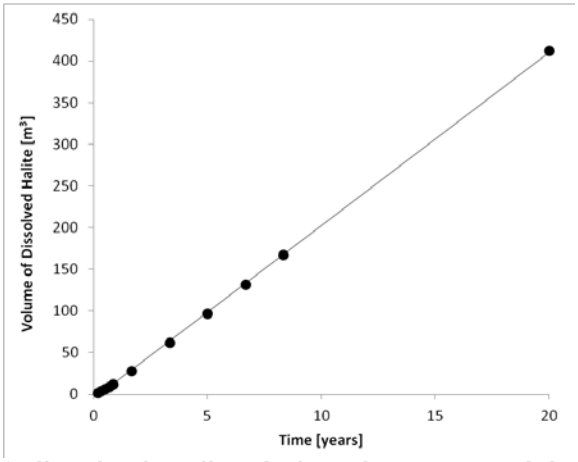

Figure 5.1: Volume of dissolved Halite during the 20 year injection period. Simulation measurements displayed as solid black circles. A linear trend line – solid black line – is added through this data ($R^2 = 0.998$).

Note, in above cavity calculations no salt creep has been assumed. It is quite possible that already within the water injection period (20 years time) salt will creep into the created cavity which will make it smaller. The cavity size indicated in Figure 5.1 should therefore be considered as a worst case scenario.

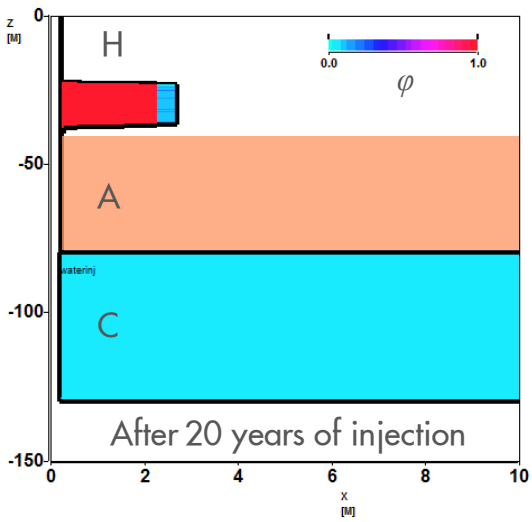

Figure 5.2: Snapshot at the end of the 20 year injection period showing the dissolution cavity within the Halite (labelled H) formation (red area, φ = 1). Injected water passes through the leak point, has a residence time within the cavity during which halite is dissolved, before passing down the cement crack through the anhydrite formation (labelled A), and into the carbonate reservoir formation (labelled C).

5.3 Scenario 3: Hydraulic fracture

Scenario 3 was modelled with a simple 3D box model (Figure 4.1) and the first dissolution script (void space modelled explicitly). This model proved to be unstable and only 1 day of water injection could be simulated. The results show dissolution occurring at the fracture-halite boundary (Figure 5.3). While the unstable nature of the simulation makes it difficult to quantify the dissolution behaviour it is likely that this scenario could lead to significant amounts of dissolved halite, as evidenced by the dissolution seen in the first day. In reality, the chance that this scenario occurs is very low because injection pressure limits have been instated for the water injection wells (NAM Report: EP201410210164). These pressure limits are sufficiently safe to avoid fracturing of the anhydrite layers, which shield off Halite formations from the injection reservoir.

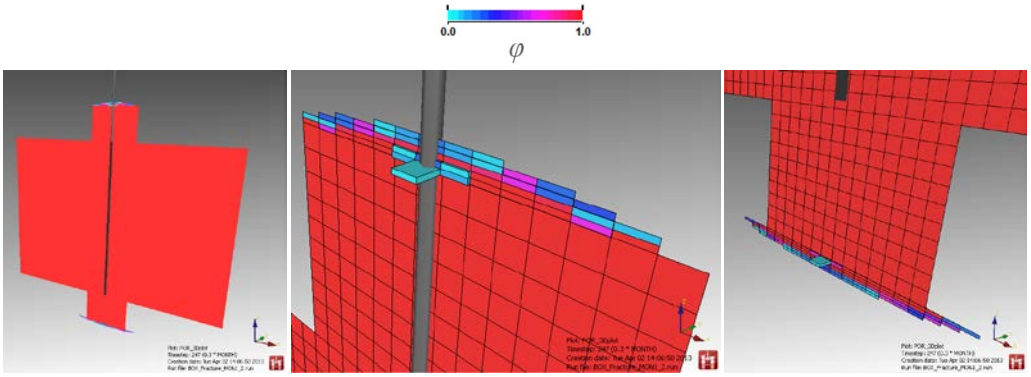

Figure 5.3: Halite dissolution at the fracture-halite boundary after 1 day of water injection. The left panel shows the full height of the wellbore fracture which passes through both carbonate and anhydrite formations. Dissolved halite cells can be made out at the upper and lower interface boundaries. Close-ups of the upper and lower interfaces are shown in the middle and right panel respectively.

5.4 Scenario 4: Water flowing past juxtaposed Halite in faulted areas

Scenario 4 investigated the situation where a fault juxtaposes halite against reservoir carbonate laterally. A number of reservoir geometry cases were investigated, these include sensitivities on the distance between injection well and fault, K_v/K_h ratio and fault throw, as summarised in Table 5.1. The model layers are (from top to base); halite, anhydrite, carbonate, anhydrite, halite. This is the same on both sides of the fault.

Note that the Carbonate reservoir is modelled as a single porosity and that therefore the ZEZ2C and ZEZ3C are modelled the same. The various cases could therefore represent ZEZ3 carbonate being juxtaposed against ZEZ3 halite, or ZEZ2 carbonate being juxtaposed against ZEZ2 halite. In addition it could also very well represent the ZEZ3 being juxtaposed against the ZEZ2.

Table 5.1: Summary of the Scenario 4 (flow past) simulation case assumptions.

Case	Distance of well from fault [m]	Fault throw [m]	Carbonate on carbonate contact across the fault	K_v/K_h	Figure
1	1000	35	15	0.001	5.4
2	1000	35	15	0.0001	5.5
3	140	35	15	0.001	5.6
4	140	35	15	0.0001	5.7
5	1000	40	10	0.001	5.8
6	1000	25	25	0.001	5.9

Initially the cases, shown in Table 5.1, were investigated with the first dissolution script (dissolution void space modelled explicitly). The simulations indicate that halite could dissolve when injection water reaches the carbonate-halite interface. Furthermore this could occur on both sides of the fault. This is displayed in Figure 5.4 (case 1) through Figure 5.9 (case 6) where dissolution void space can be identified by imperfections in the vertical fault plane at Z = -75 m and between Z = -110 to -135 m at X = 2000 m. Reducing the K_v/K_h ratio by a factor 10 (cases 2 and 4) (Figures 5.5 and 5.7) significantly impacts the ability of injection water to flow across a fault and up to the halite interval. Furthermore dissolution in the fault block containing the injection well is also reduced due to changes to the local flow field near the fault (less vertical flow). The well location is also shown to have an impact on dissolution; when the well is closer to the fault more halite dissolution was predicted in the simulation cases (see Figures 5.6 and 5.7).

Finally the impact of fault throw is considered. The throw of the fault will determine the height of carbonate on carbonate contact across the fault. A range of fault throws were investigated, ranging from 25 to 40 m (corresponding to a carbonate contact height range of 10 to 25 m). The results show that the larger the throw (smaller the carbonate contact height) the greater the halite dissolution (see figures 5.4, 5.8 and 5.9)

It should be noted that at the fault interface a direct undisturbed contact has been assumed between the lithologies. In reality a reduction in permeability in the Carbonate layers near faults can be expected as salt creep causes fractures in the vicinity of the fault to be filled with salt. This will reduce cross-flow past faults and will therefore significantly hamper halite dissolution near faults.

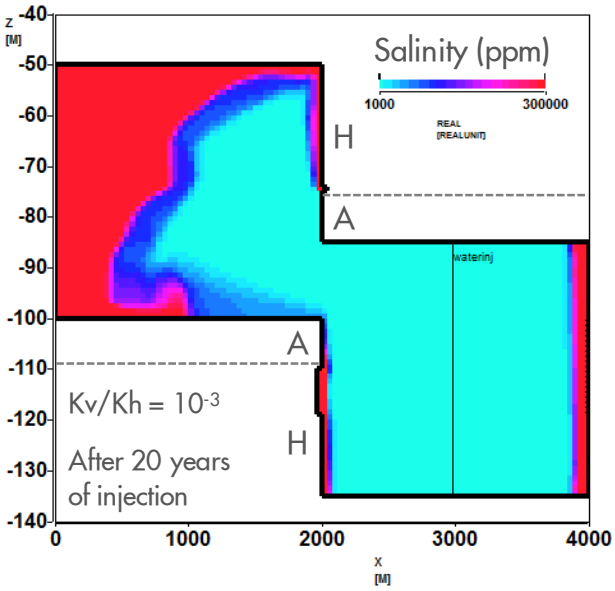

Figure 5.4: Cross-section through the scenario 4, case 1 Dynamo-MoReS box model after 20 years of water injection. K_v/K_h = 1 × 10^{-3}. The water salinity in the reservoir pore space is displayed. The water injection well is located in the right hand fault block (X = 3000 m), 1000 m from the fault.

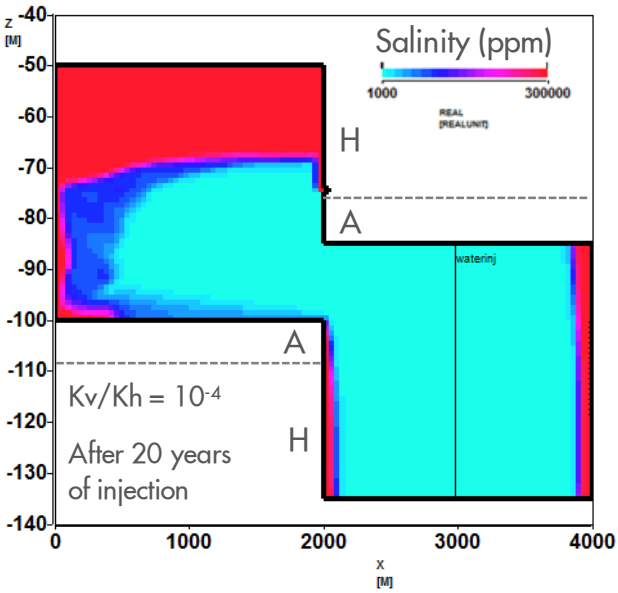

Figure 5.5: Cross-section through the scenario 4, case 2 Dynamo-MoReS box model after 20 years of water injection. K_v/K_h = 1 × 10^{-4}. The water salinity in the reservoir pore space is displayed. The water injection well is located in the right hand fault block (X = 3000 m) , 1000 m from the fault.

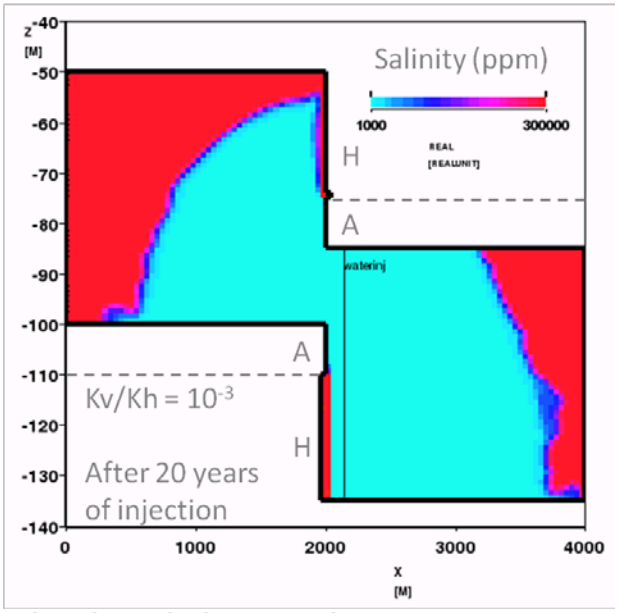

Figure 5.6: Cross-section through the scenario 4, case 3 Dynamo-MoReS box model after 20 years of water injection. K_v/K_h = 1 × 10^{-3}. The water salinity in the reservoir pore space is displayed. The water injection well is located in the right hand fault block (X = 2140 m) , 140 m from the fault.

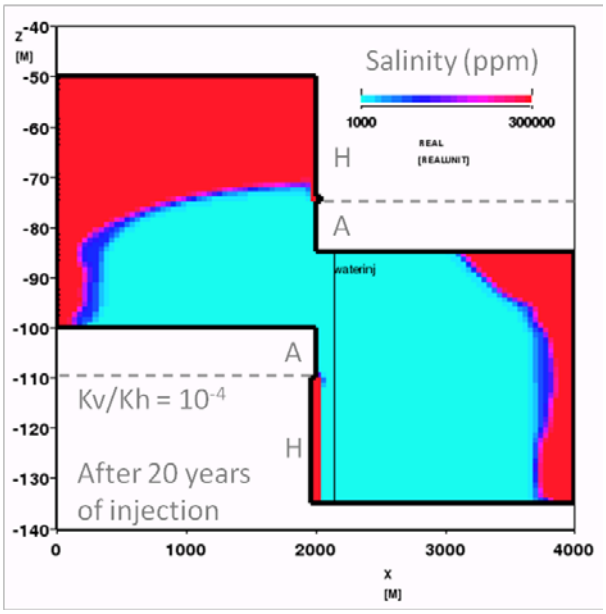

Figure 5.7: Cross-section through the scenario 4, case 4 Dynamo-MoReS box model after 20 years of water injection. K_v/K_h = 1 × 10^{-4}. The water salinity in the reservoir pore space is displayed. The water injection well is located in the right hand fault block (X = 2140 m) , 140 m from the fault.

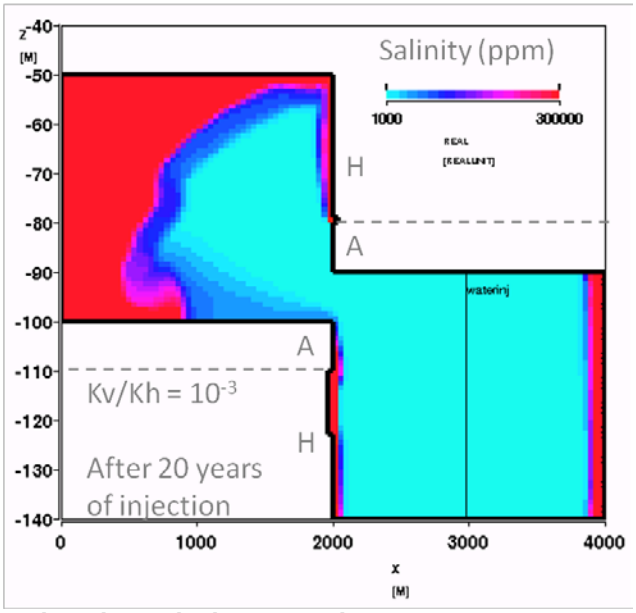

Figure 5.8: Cross-section through the scenario 4, case 5 Dynamo-MoReS box model after 20 years of water injection. K_v/K_h = 1 × 10^{-3}. The water salinity in the reservoir pore space is displayed. The water injection well is located in the right hand fault block (X = 3000 m) , 1000 m from the fault. The carbonate on carbonate contact across the faul is reduced to 10 m.

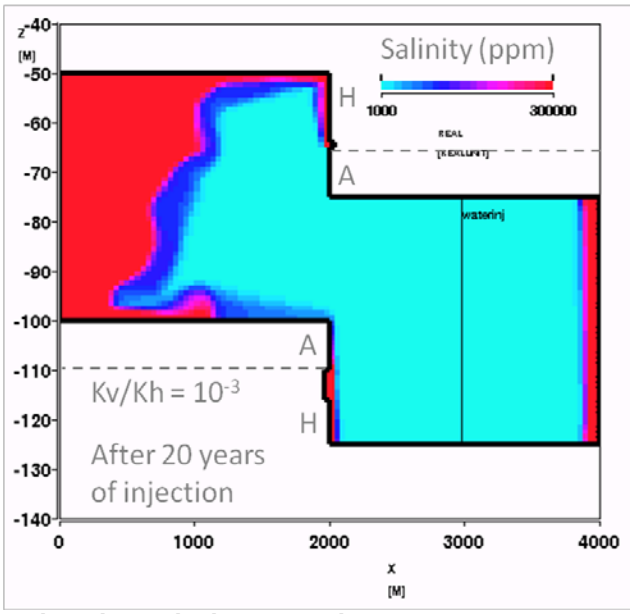

Figure 5.9: Cross-section through the scenario 4, case 6 Dynamo-MoReS box model after 20 years of water injection. K_v/K_h = 1 × 10^{-3}. The water salinity in the reservoir pore space is displayed. The water injection well is located in the right hand fault block (X = 3000 m) , 1000 m from the fault. The carbonate on carbonate contact across the faul is increased to 25 m.

To investigate post injection behaviour – specifically the possibility of convective flow loops developing – an additional simulation was performed using the second halite dissolution script (Section 2.4.2). Here a box model is filled with fresh water and the dissolution script is applied to one part of a side face of the model (Figure 5.10). Properties are assumed to be homogenous with a Kv/Kh of 1. The modelling shows that there is a rapid onset of convection (Figure 5.11 a-c) but only very localised dissolution: halite saturated water slumps to the bottom of the model causing a maximum dissolution of the order of 0.3 m after 1.9 years at the very top of the formation, with this dissolution distance decreasing quickly away from the top of the model (Figure 5.11).

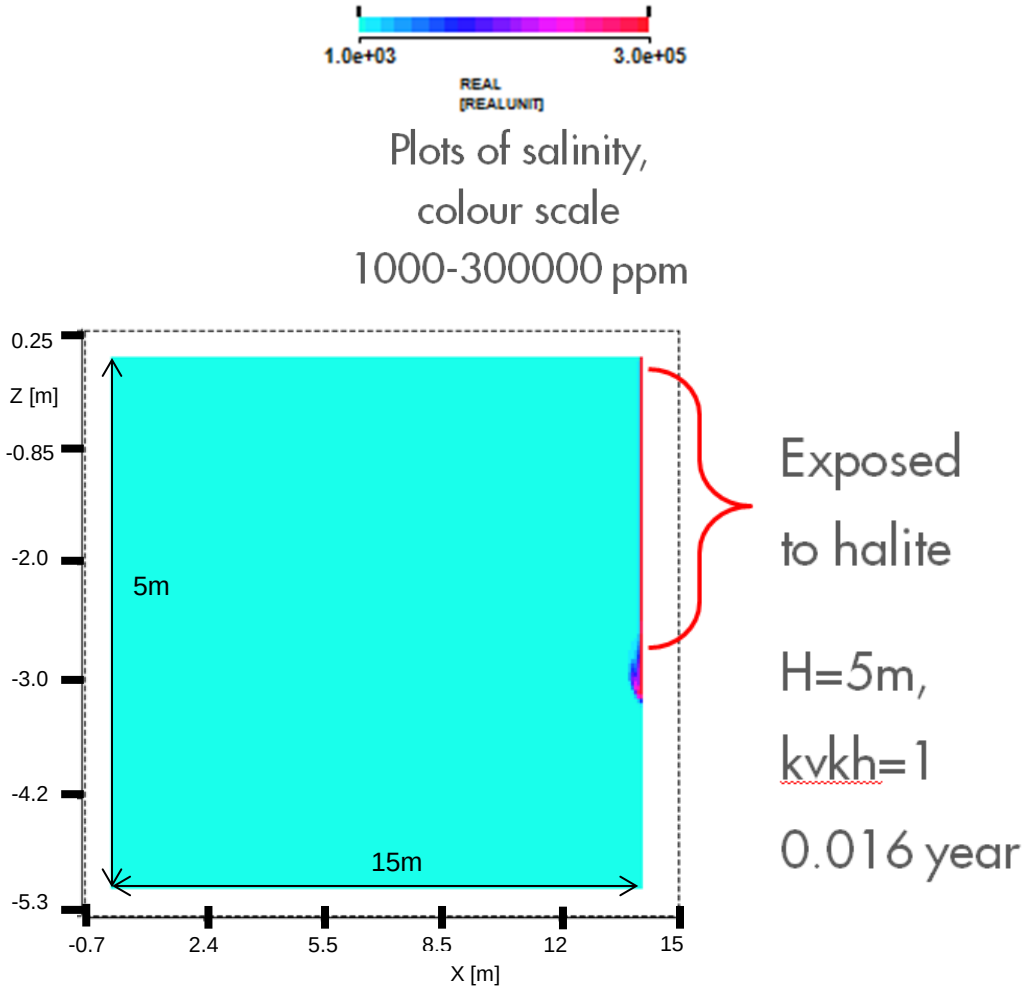

Figure 5.10: Box model utilising the second dissolution script used to investigate post injection convective mixing behaviour. Kv/Kh is set at 1. Water salinity is shown after 0.016 years and the onset of convection is visible as a change to the salinity colour scale in proximity to the segment of the right model face exposed to halite.

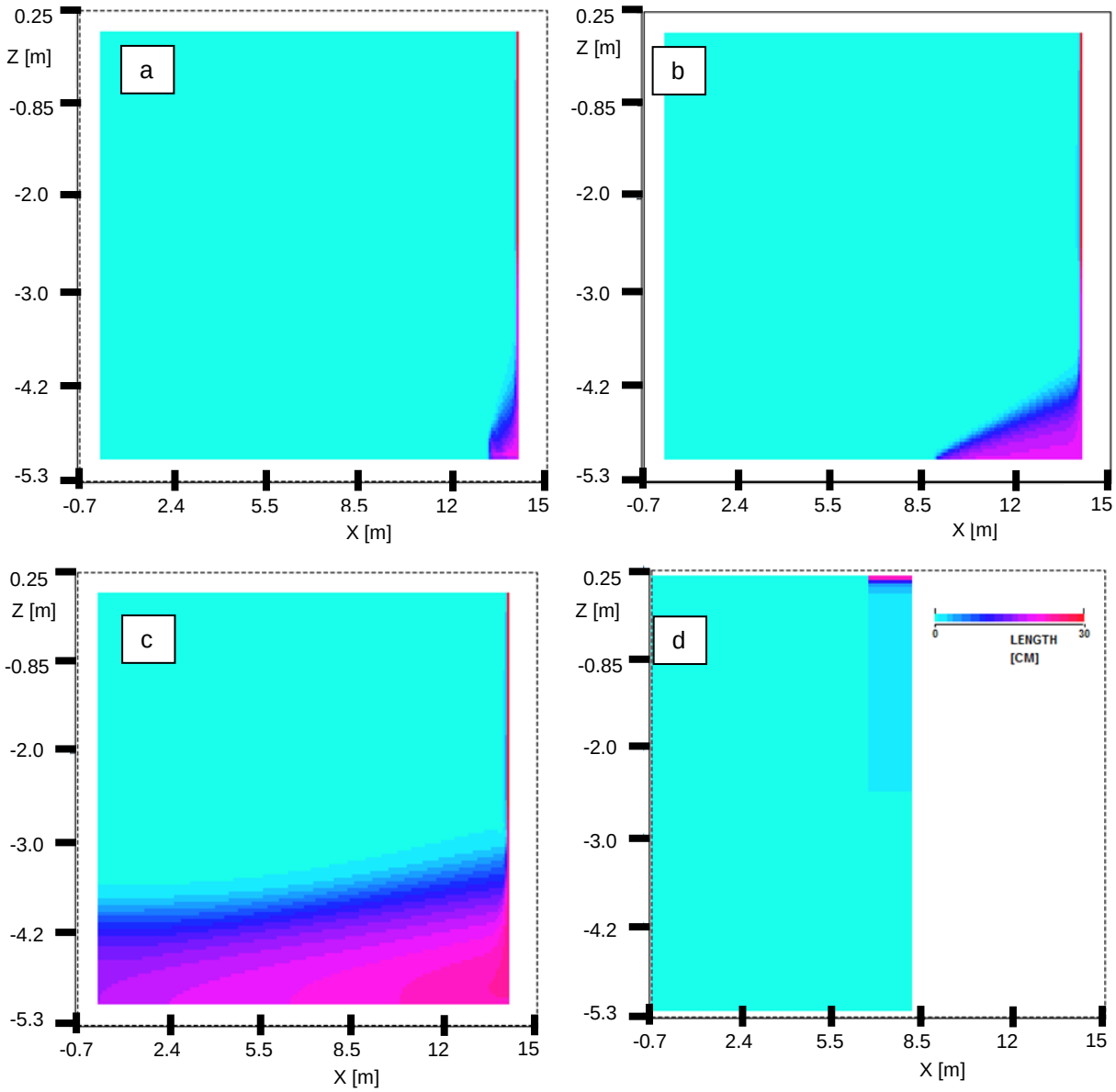

Figure 5.11: Salinity change over time caused by density driven convection. Part of the left face of the box model is designated as halite. Low salinity brine in proximity with this face is halite saturated, the resulting density increase driving convection. Salinity shown after 0.065 years (a), 0.23 years (b), and 1.9 years (c). The resulting amount of halite dissolved (expressed as a dissolution distance) is shown (d), the maximum dissolved distance is of the order 0.3 m at the top of the box model.

A coarser grid model was subsequently run to check the effect over a much longer time (i.e. thousands of years). The results are shown in Figure 5.12a where the dissolution distance into the Halite side face is given as a function of the height from the top of the Carbonate cell (see also Figure 5.10 – to the top right the 5m high Carbonate cell, filled with fresh water, has been exposed to 2.5m of Halite). This figure shows that after 23,200 years only 4m of salt at the top of the Carbonate cell and 1.5m at the middle of the Carbonate cell (i.e. bottom of exposed Halite) has been dissolved.

The coarser grid model has also been run for a Kv/Kh of 0.001. The results are shown in Figure 5.12b. This figure shows similar dissolution distances as for the Kv/Kh =1 case (although the Kv/Kh =1 case shows a somewhat more preferential dissolution at the top versus the bottom of the exposed Halite). This suggests that the dissolution distance is insensitive to Kv/Kh. For 232,000 years the Kv/Kh =0.001 case shows a maximum dissolution distance of 6m only.

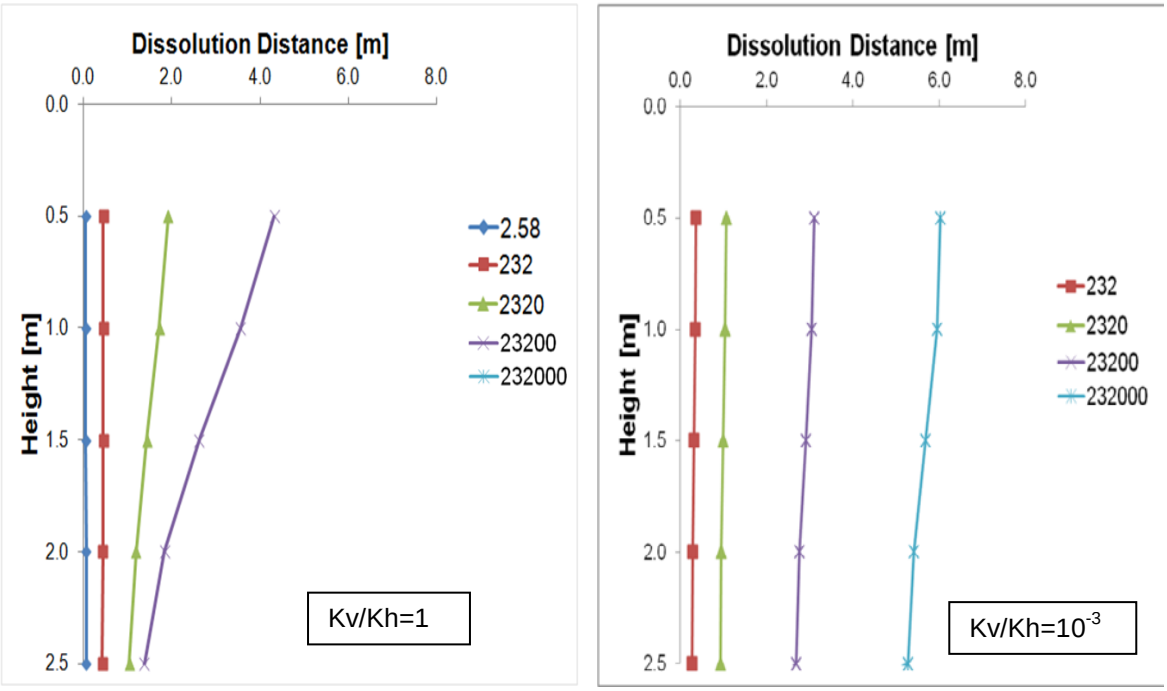

5.12a 5.12b

Figure 5.12: Dissolution front distance into Halite as a function of distance from top of Carbonate cell. Figure 5.12a shows results for Kv/Kh =1 and Figure 5.12b for Kv/Kh =0.001. Note, the 232,000yr case for Kv/Kh =1 did not run due to slow computing time.

5.5 Scenario 5: Convection

In scenario 5 a range of convection cases were simulated to investigate the timescale of dissolution for different heights and permeabilities (K_v/K_h). These cases were based on our understanding of the ZEZ3C and ZEZ2C properties as outlined in Section 2. To recap, the ZEZ3C features 0.2-0.3 m thick fractured carbonate intervals interspersed with unfractured anhydrite layers, while the ZEZ2C comprises more massive alternating (unfractured) anhydrite and (fractured) carbonate intervals of the order of 4-5m thickness each.

Based on this geological understanding cases with 3 different heights were investigated. These are 0.3m, 5m and 50m where 0.3m corresponds to a ZEZ3C fractured carbonate sub-layer, 5m to a ZEZ2C fractured carbonate sub-layer and 50m to the total Carbonate interval (including interspersed Anhydrite).

For the 0.3m case a Kv/Kh =1 case was investigated as the vertical fracture dimensions are expected to be equal to the vertical height of these flow units. For the 5m case a Kv/Kh range of 0.001 to 1.0 was studied. These endpoints were chosen to study the entire potentially possible Kv/Kh range for this flow unit, however it should be noted that a Kv/Kh =1 case becomes less likely when the flow units inside the Carbonate formation become thicker. For the 50m case a range of 0.01 to 0.001 was investigated. Herewith note that, as mentioned in Section 2.1, on a reservoir scale (i.e. the 50m thick Carbonate interval consisting of fractured Carbonate layers interspersed with Anhydrite layers) the Kv/Kh ratios are expected to range from 0.005 for an unfaulted area to 0.0001 for areas, affected by fault associated fractures.

The cases were simulated in 2D box models and are summarised in Table 5.2. In addition one 3D box model was made to validate the 2D results.

Table 5.2: Cases simulated to investigate convection driven halite dissolution (dissolution scenario 5). A range of heights and permeability ratios were considered based on the uncertainty associated with the geology of the ZEZ3C and ZEZ2C formations.

Convection Case	2D Model Height (m)	K_v/K_h ratio	Notes
1	0.3	1.0	ZEZ3C carbonate sub-layer, high perm ratio due to lack of anhydrite intra-layers
2	5	0.001	ZEZ2C carbonate sub-layer, low perm ratio to investigate best case scenario for convection
3	5	1.0	ZEZ2C carbonate sub-layer, high perm ratio represents current geologic interpretation with no anhydrite intra-layers within the carbonate interval
4	50	0.001	Entire ZEZ3C or ZEZ2C fm., low permeability ratio represents the presence of anhydrite intra-layers
5	50	0.01	Entire ZEZ3C or ZEZ2C fm., high perm ratio investigated as a worst case scenario for convection driven dissolution

In the first simulation case – a 0.3 m thick model with a K_v/K_h ratio of 1.0 – convective patterns do not fully develop, the salinity front reaches the bottom of the model before this can occur. Indeed diffusion alone is sufficient to achieve full mixing within 3 years ($t = H^2/D$). The halite dissolution capacity of such a carbonate sub layer is approximately 0.001 m ($H \times 0.03 \times 0.8 / 7 = 0.0034H$). Figure 5.13 illustrates the salinity distribution within the box model after 0.17 years when the salinity front reaches the model base.

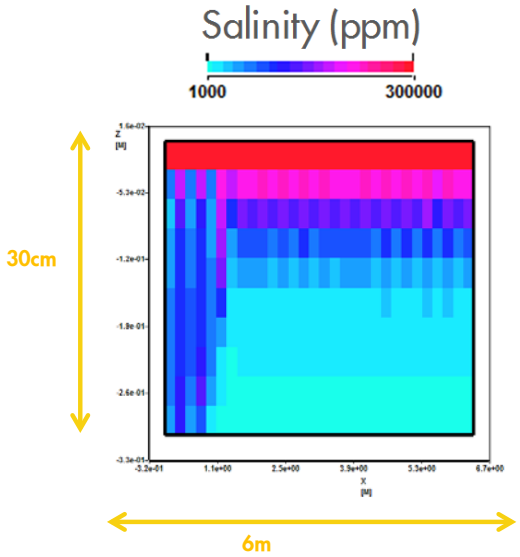

Figure 5.13: Box model of the 0.3 m, K_v/K_h ratio of 1.0, simulation case. Diffusion alone is sufficient for the salinity front to reach the base of the model. Convective patterns do not fully develop and are not required for full mixing.

The second and third simulation cases – a 5 m thick model with K_v/K_h ratios of 0.001 and 1.0 – illustrate the important role that the permeability ratio plays. Similar to the previous case, the K_v/K_h = 0.001 case shows that the advance of the salinity front is diffusion controlled: convective patterns do not form by the time the front reaches the base of the model (Figure 5.14). In contrast the K_v/K_h = 1.0 case features the development of classical convective mixing patterns (teardrop effect – Figure 5.15). At early time the advance of the salinity front is diffusion dominated (Figure 5.15a), subsequently gravitational instabilities result in the onset of convective patterns (Figure 5.15b) after 0.13 years. After 0.23 years the convective patterns are fully developed (Figure 5.15c) and after 0.66 years they reach the base of the model (Figure 5.15d). The convective mixing continues until all of the water is fully

halite saturated, although the rate of salinity increase decreases with time as the density difference decreases (Figure 5.16). In both of these cases there is the capacity to dissolve approximately 0.017 m of halite across the top surface of the models.

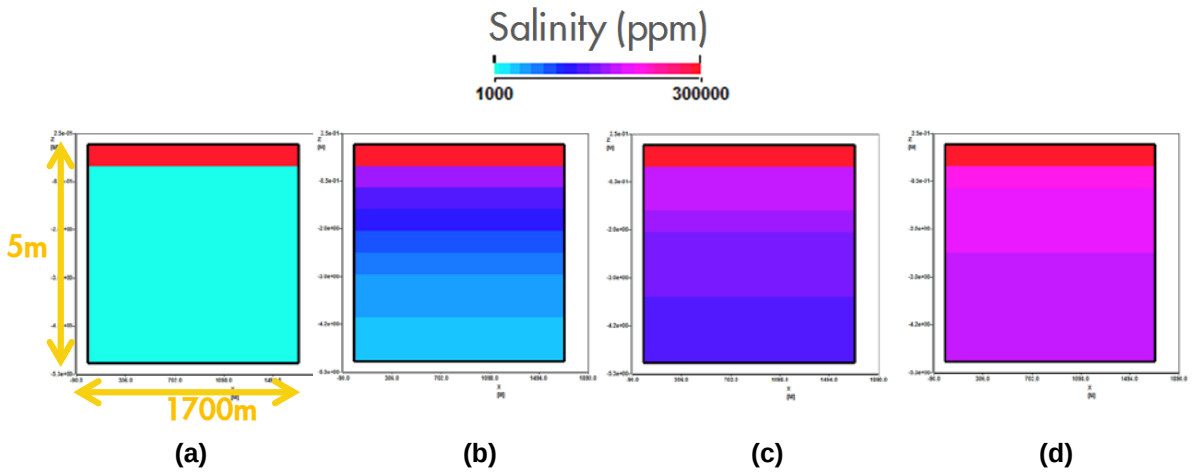

Figure 5.14: Box model of the 5 m, K_v/K_h ratio of 0.001, simulation case. Salinity shown after 6.6 years (a), 200 years (b), 1000 years (c), and 2000 years (d). Diffusion alone is sufficient for the salinity front to reach the base of the model.

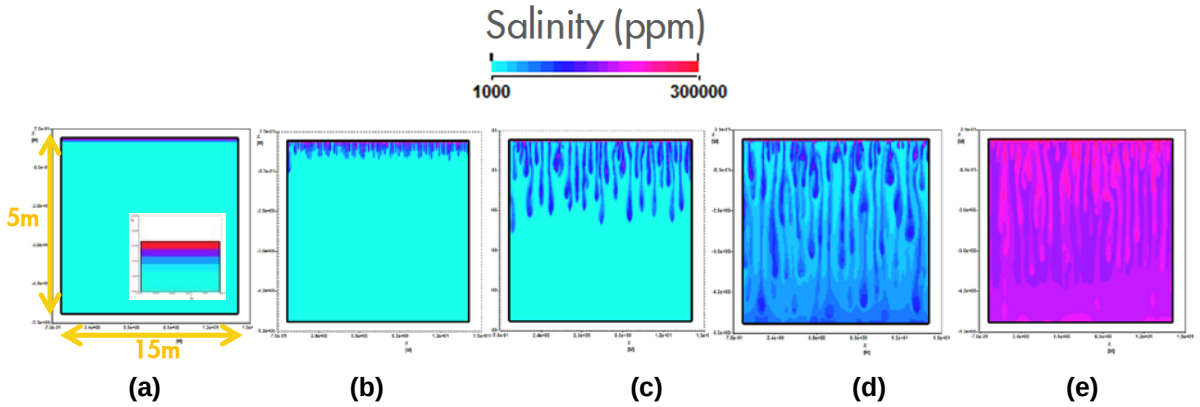

Figure 5.15: Box model of the 5 m, K_v/K_h ratio of 1.0, simulation case. Salinity shown after 0.07 years (including an inset showing the top 0.3 m of the model) (a), 0.13 years (b), 0.23 years (c), 0.66 years (d), and 4.47 years (e). Classical, fully developed, convective mixing patters are evident after the early, diffusion dominated, period (a).

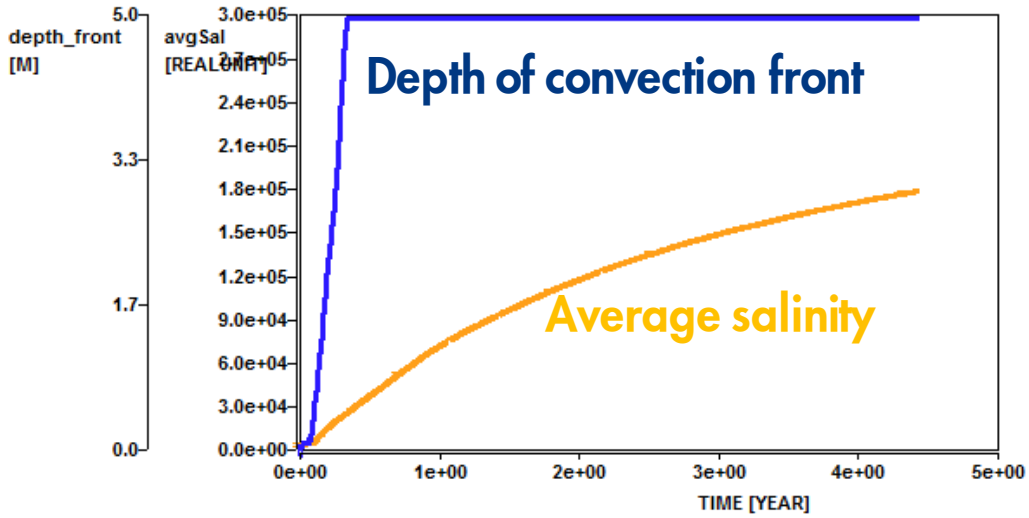

Figure 5.16: Depth of the convection (salinity) front (y-axis title: depth_front) and the average salinity (y-axis title: avgSal) versus time for the 5 m, K_v/K_h ratio of 1.0, simulation case.

The final convection cases consider a 50 m thick carbonate interval which has the capacity to dissolve 0.17 m of halite from the top surface of the box model. Again the timescale of dissolution is controlled by the permeability ratio. For a K_v/K_h ratio of 0.001 the same behaviour is initially seen as in the 5 m case with the same permeability ratio. However, since the length scale (height) is larger, convective patterns develop later: since the model height is now larger these patterns form at a depth greater than 5 m, hence why they were not seen in the 5 m case. This is shown in Figure 5.17. In the final case – K_v/K_h ratio of 0.01 –convective patterns are formed earlier due to the smaller permeability ratio (Figure 5.18).

As in the 5 m case the front depth salinity is plot versus time (Figure 5.19). In both cases the average salinity is approximately 30,000 ppm when the front reaches the base. If the average salinity is plot against a scaled time axis then both cases (5m and 50m cases) are nearly identical (Figure 5.20), with the scaling parameters being proportional to the characteristic time to the onset of convection (determined from analytical equations as described in section 4.5).

One 3D box model was made to allow comparison and validation of the 2D results with 3D results. The 2D model reproduces the characteristic time and length scales of the 3D model as shown in Figure 5.21 and Figure 5.22.

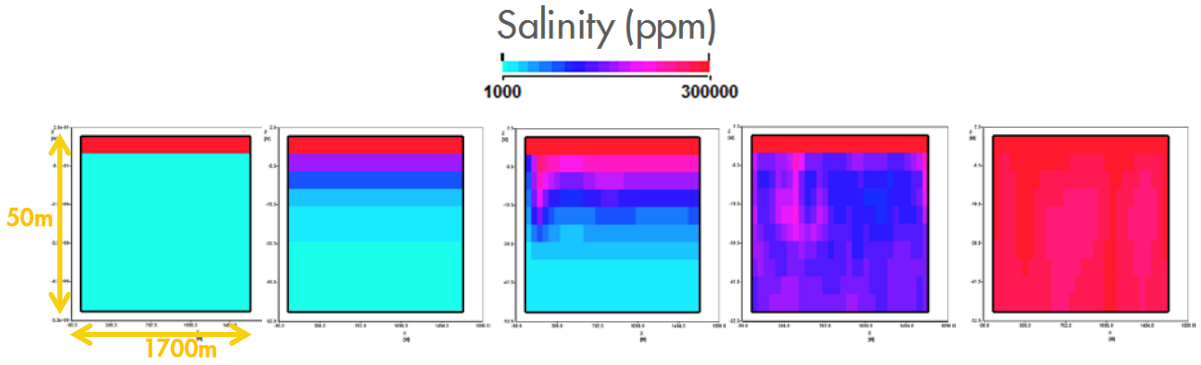

(a) (b) (c) (d) (e)

Figure 5.17: Box model of the 50 m, K_v/K_h ratio of 0.001, simulation case. Salinity shown after 6.6 years (a), 2000 years (b), 8000 years – onset of instability – (c), 12000 years (d), and 50000 years (e).

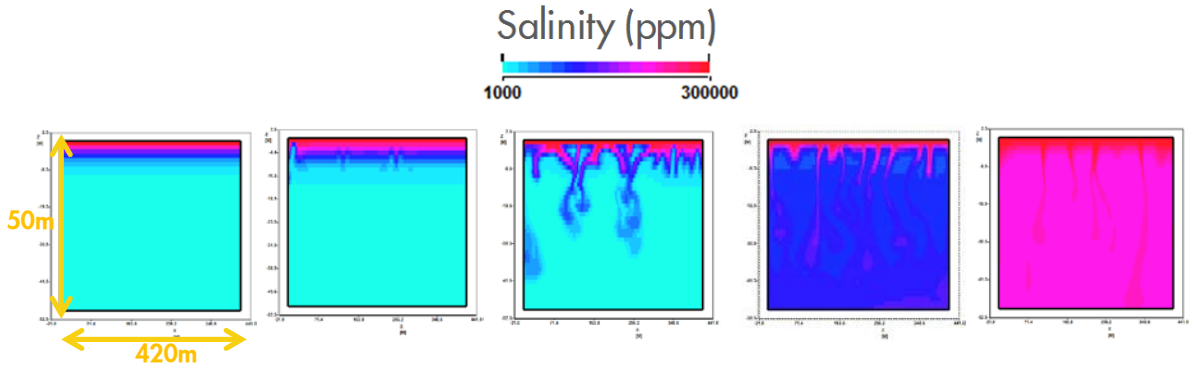

(a) (b) (c) (d) (e)

Figure 5.18: Box model of the 50 m, K_v/K_h ratio of 0.01, simulation case. Salinity shown after 300 years (a), 600 years – onset of instability – (b), 750 years (c), 3000 years (d), and 12000 years (e).

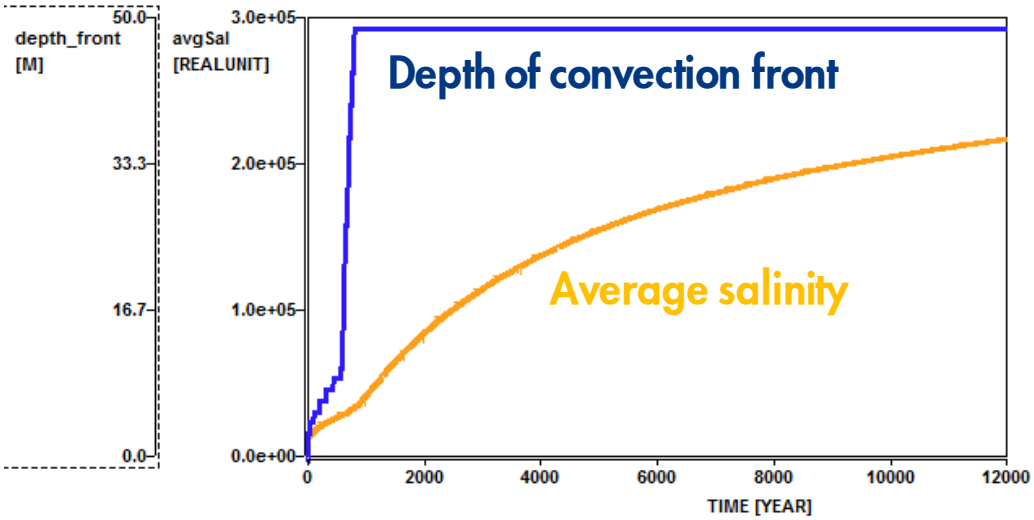

Figure 5.19: Depth of the convection (salinity) front (y-axis title: depth_front) and the average salinity (y-axis title: avgSal) versus time for the 50 m, K_v/K_h ratio of 0.01, simulation case.

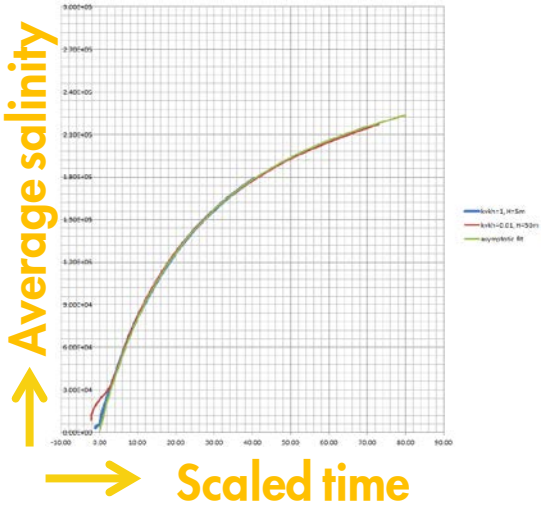

Figure 5.20: Average salinity data from the 5 m and 50 m box model simulations versus scaled time. Curves are almost identical and can be fitted with a simple function.

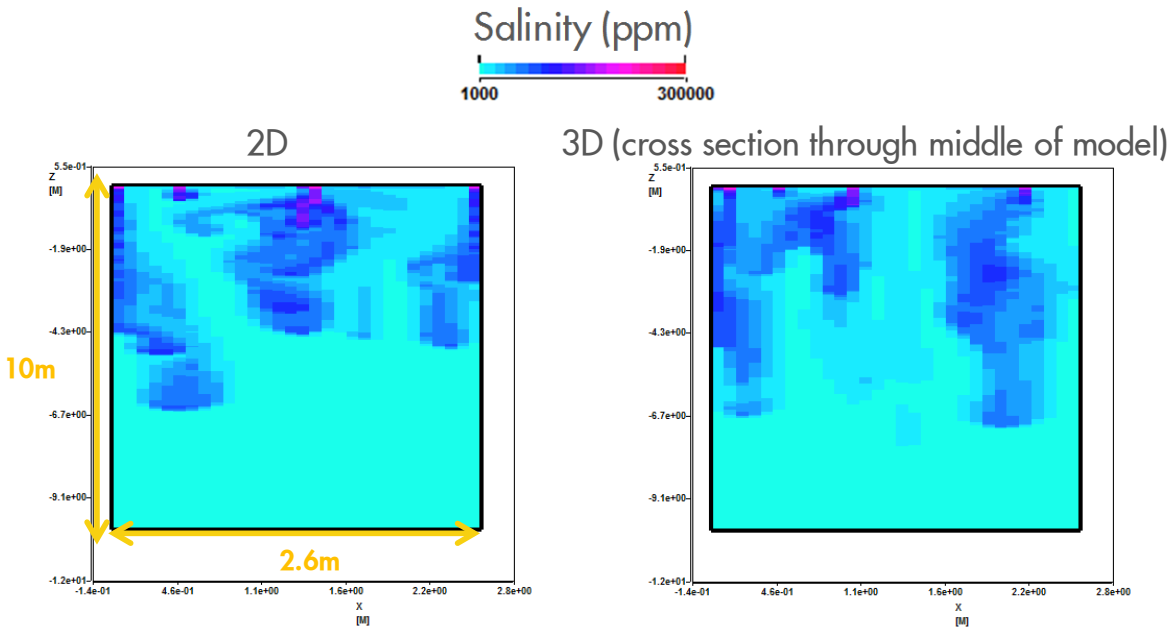

Figure 5.21: Comparison of 2D and 3D box models. Model height is 10 m and K_v/K_h is 1.0 in both cases with the salinity distribution shown after time 2 months. The slice from the 3D model is a cross-section through the middle of the model.

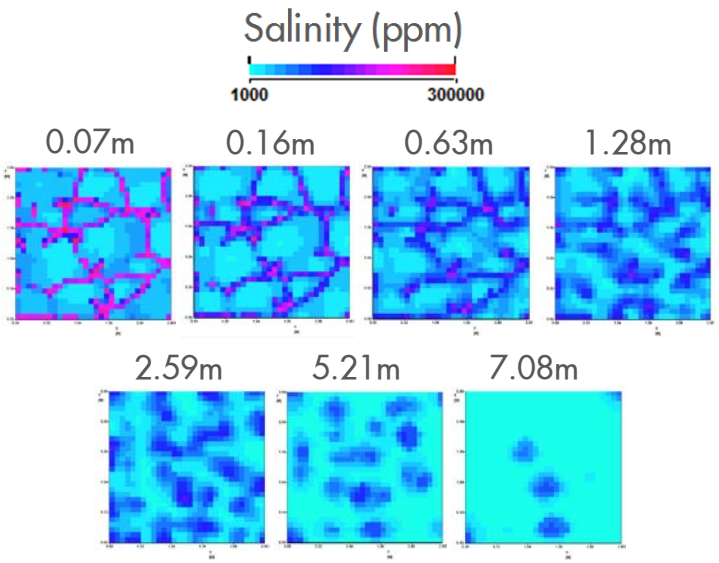

Figure 5.22: XY map view showing the salinity distribution at various depths through the 3D box model.

In addition to the numerical work also an analytical analysis has been made. Herewith use has been made of the equations (8) – (10) in section 4.5. These equations give estimates for the critical time (t_c) – that is the time at which an instability begins to propagate – the dimensional critical wavelength (λ_c) and the penetration depth at the onset of instability (δ_c).

Results from the analytical equations, which have been summarised in Table 5.3 below, agree well with the numerical results shown above. This allows combining the numerical and analytical results. Figure 5.20, which shows numerical output, then can be used to derive the required time $t_{150,000}$ to reach an average salinity of 150,000ppm NaCl (note fully saturated water contains approximately 300,000-320,000ppm NaCl). As mentioned above this figure shows an identical curve for the average salinity for several cases (5m and 50m cases) as a function of scaled time – with the analytical parameters t_c, λ_c, and δ_c as the scaling parameters. Calculating these analytical parameters thus allows the time $t_{150,000}$ to be derived from Figure 5.20. These $t_{150,000}$ results have also been given in Table 5.3, which shows that it takes a significant long time for convection cells in low Kv/Kh 50m Carbonate cells to saturate water up to 150,000ppm salinity. For a Kv/Kh of 10^{-3} it takes close to

8,000years to achieve an average salinity of 150,000ppm whilst for a Kv/Kh of 10^{-4} it even takes close to 75,000years to achieve this.

Table 5.3: Summary of analytical estimates of finger spacing and time to reach an average salinity of 150000 ppm.

H	φ	μ_w	D	K_h	K_v/K_h	S_w	$\Delta\rho$	finger spacing	time to reach avg. salinity of 150000ppm	diffusion dominated?
m	*frac*	*cP*	*m2/s*	*mD*	*frac*	*frac*	*kg/m3*	*m*	*yr*	*boolean*
0.3	0.03	1.6	1E-09	177	1.0000	0.85	210	1.0	0.2	FALSE
0.3	0.03	1.6	1E-09	177	0.1000	0.85	210	4.2	0.8	FALSE
0.3	0.03	1.6	1E-09	177	0.0100	0.85	210	29.5	2.9	TRUE
0.3	0.03	1.6	1E-09	177	0.0010	0.85	210	259.5	2.9	TRUE
0.3	0.03	1.6	1E-09	177	0.0001	0.85	210	2487.1	2.9	TRUE
5	0.03	1.6	1E-09	177	1.0000	0.85	210	1.0	2.9	FALSE
5	0.03	1.6	1E-09	177	0.1000	0.85	210	4.2	12.7	FALSE
5	0.03	1.6	1E-09	177	0.0100	0.85	210	29.5	88.4	FALSE
5	0.03	1.6	1E-09	177	0.0010	0.85	210	259.5	777.9	FALSE
5	0.03	1.6	1E-09	177	0.0001	0.85	210	2487.1	792.7	TRUE
50	0.03	1.6	1E-09	177	1.0000	0.85	210	1.0	29.2	FALSE
50	0.03	1.6	1E-09	177	0.1000	0.85	210	4.2	126.6	FALSE
50	0.03	1.6	1E-09	177	0.0100	0.85	210	29.5	884.4	FALSE
50	0.03	1.6	1E-09	177	0.0010	0.85	210	259.5	7778.8	FALSE
50	0.03	1.6	1E-09	177	0.0001	0.85	210	2487.1	74561.8	FALSE

6. Conclusions & Discussion

In this report Halite dissolution modelling is being discussed, which has been performed to check the dissolution effects of low saline water injection into depleted Carbonate gas reservoirs containing a Halite cap and base rock.

From the modelling it is apparent that the risk for and impact of Halite dissolution is very low.

Halite dissolution can only occur when low saline injection water is able to connect to and flow directly past Halite rock. Based on a review of the injection well design and the injection reservoir geology, it is identified that there may only be a few very specific situations where such a “Halite flow past scenario” could occur. These have been investigated in more detail using numerical flow simulations to get a better understanding of the dissolution risk and impact.

It is shown that injection into a wellbore with a casing leak in combination with a poor quality wellbore cement could, if left undetected for many years, lead to local, near-wellbore, salt dissolution. There is however an extensive well monitoring program in place to ensure that occurrence of such conditions is avoided or detected early (Ref NAM Report: EP201410210164).

A hydraulic fracture in the reservoir that grows over time may have the potential of bringing significant quantities of injection water in contact with the over- and/or under-lying halite layers resulting in dissolution. However, the chance that this scenario occurs is very low because injection pressure limits have been instated for the water injection wells that will prevent the formation and growth of hydraulic fractures (Ref NAM Report: EP201410210164). In addition, the mechanical contrast between the brittle carbonates and the plastic anhydrites is such that growth of hydraulic fractures will be arrested at the interface.

Juxtaposition of halite against carbonate across a fault could result in low saline water flowing past juxtaposed halite formations. However, modelling shows that significant Halite dissolution is not expected, in view of the presence of unfractured anhydritic layers which are interspersed in the fractured Carbonate reservoirs. This renders the vertical communication inside the Carbonate reservoir to be very low (K_v/K_h is assumed to be in the range of 10^{-3} to 10^{-4}). In addition the geological data (NAM Report: EP201310201845) has shown that the permeability close to the fault zones is severely downgraded because of salt creep blocking the high perm natural fractures. The net effect is that any low saline water reaching the faultzone cannot flow away sufficiently fast and in sufficient quantities to cause significant dissolution.

Finally, modelling of the down-dip flanks areas of the injection reservoir has shown that it takes thousands of years for convection loops to develop at reservoir scale (i.e. 50m thickness). This is again due to a very low expected vertical communication within the Carbonate reservoir (K_v/K_h is in the range of 10^{-3} to 10^{-4}). Simulations show that it will take 8000 to 75000 years for a convective loop to develop. In addition the total dissolution capacity of such a convection loop was found to be limited (a convection loop within 50m Carbonate reservoir is expected to be able to dissolve 0.17 m overlying Halite formation).

The overall conclusion is is in line with the original EIA. The risk for significant salt dissolution to occur in settings like in the Twente disposal fields is very small. The biggest exposure could occur in the near well bore region if leak points in poorly cemented casing opposite halite layers would remain undetected for a long time (many years). The well integrity monitoring programme implemented in Twente prevents this from happening.

8. References

Dean, J.A. 1999. *Lange's Handbook of Chemistry (15th Edition).* s.l. : McGraw-Hill, 1999.

Onset of Convection in a Gravitationally Unstable Diffusive Boundary Layer in Porous Media. **Riaz, A., et al. 2006.** 2006, J. Fluid Mech., Vol. 548, pp. 87-111.

Permeability and porosity models considering anisotropy and discontinuity of coalbeds and application in coupled simulation. **Gu, Fagang and Chalaturnyk, Rick. 2010.** 3-4, 2010, Journal of Petroleum Science and Engineering, Vol. 74, pp. 113-131.

Rate of Dissolution due to Convective Mixing in the Underground Storage of Carbon Dioxide. **Ennis-King, J. and Paterson, L. 2003.** 2003, Greenhouse Gas Control Technologies, Vol. 1, pp. 507-210.

*Geology description of Twente Gas Fields: Tubbergen, Tubbergen-Mander and Rossum-Weerselo***.** NAM Report: EP201310201845

Technical evaluation of Twente water injection wells ROW3, ROW4, ROW7, ROW9, TUB7 and TUB10 3 years after start of injection NAM Report: EP201410210164

Smits, R.M.M and Jing, X.D. 2003. *EP 2003-5041: A relative permeability database for water / oil imbibition in sandstone and carbonate reservoirs.* Rijswijk : Shell International Exploration and Production B.V., 2003.

Warren, Geoff and Bisschop, Radboud. 2006. *EPE200401201716: Schoonebeek Oilfield Redevelopment VAR 3 Field Development Plan Updated Final Version.* Assen, The Netherlands : NAM, 2006.

Weijermans, P.J. 2004. *Schoonebeek Produced Water Disposal Study: Dynamic Modelling of Water Injection in Depleted Naturally Fractured Zechstein Carbonates.* s.l. : Horizon Energy Partners, 2004.

Hagoort, J.: *"Productivity index of a well in a dual-porosity reservoir", paper submitted for publication in the SPEREE, May 2003*